Accepted Manuscript

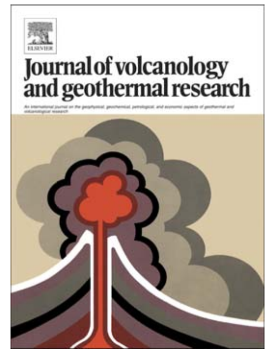


# Long-term changes in explosive and effusive behaviour at andesitic arc volcanoes: Chronostratigraphy of the Centre Hills Volcano, Montserrat

Maya Coussens, Michael Cassidy, Sebastian F.L. Watt, Martin Jutzeler, Peter J. Talling, Dan Barfod, Thomas M. Gernon, Rex Taylor, Stuart J. Hatter, Martin R. Palmer

PII: S0377-0273(17)30012-4
DOI: doi:10.1016/j.jvolgeores.2017.01.003
Reference: VOLGEO 5982

To appear in: *Journal of Volcanology and Geothermal Research*

Received date: 12 February 2016
Revised date: 15 December 2016
Accepted date: 2 January 2017

Please cite this article as: Coussens, Maya, Cassidy, Michael, Watt, Sebastian F.L., Jutzeler, Martin, Talling, Peter J., Barfod, Dan, Gernon, Thomas M., Taylor, Rex, Hatter, Stuart J., Palmer, Martin R., Long-term changes in explosive and effusive behaviour at andesitic arc volcanoes: Chronostratigraphy of the Centre Hills Volcano, Montserrat, *Journal of Volcanology and Geothermal Research* (2017), doi:10.1016/j.jvolgeores.2017.01.003

**Long-term changes in explosive and effusive behaviour at andesitic arc volcanoes: chronostratigraphy of the Centre Hills Volcano, Montserrat**

**Maya Coussens**
School of Ocean and Earth Science, National Oceanography Centre, University of Southampton, European Way, Southampton, SO14 3ZH, UK (maya.pratt@mail.com)

**Michael Cassidy**
Institute of Geosciences, Johannes Gutenberg, University Mainz, J- J- Becher- Weg 21, D-55128, Mainz, Germany (mcassidy@uni-mainz.de)

**Sebastian. F. L. Watt**
School of Geography, Earth and Environmental Sciences, University of Birmingham, Edgbaston, Birmingham, B15 2TT, UK (s.watt@bham.ac.uk)

**Martin Jutzeler**
School of Physical Sciences and Centre of Excellence in Ore Deposits (CODES), University of Tasmania, Hobart TAS 7001, Australia (jutzeler@gmail.com)

**Peter. J. Talling**
National Oceanography Centre, Southampton, University of Southampton, Southampton S014 3ZH, UK (peter.talling@noc.ac.uk)

**Dan Barfod**
Scottish Universities Environmental Research Centre, Rankine Avenue, Scottish Enterprise Technology Park, East Kilbride, G75 0QF, UK (Dan.Barfod@glasgow.ac.uk).

**Thomas. M. Gernon, Rex Taylor, Stuart. J. Hatter, Martin. R. Palmer**
School of Ocean and Earth Science, National Oceanography Centre, University of Southampton, European Way, Southampton, SO14 3ZH, UK (Thomas.Gernon@noc.soton.ac.uk), (rex@noc.soton.ac.uk), (sjh1e13@soton.ac.uk), (m.palmer@noc.soton.ac.uk)

**and the Montserrat Volcano Observatory**
Mongo Hill, Montserrat, PO Box 318, Flemmings, Montserrat, West Indies

**Abstract**
Volcanism on Montserrat (Lesser Antilles arc) has migrated southwards since the formation of the Silver Hills ~2.5 Ma, and has formed three successively active volcanic centres. The Centre Hills volcano was the focus of volcanism from ~1–0.4 Ma, before activity commenced at the currently active Soufrière Hills volcano. The history of activity at these two volcanoes provides an opportunity to investigate the pattern of volcano behaviour on an andesitic arc island over the lifetime of individual volcanoes. Here, we describe the pyroclastic stratigraphy of subaerial exposures around central Montserrat; identifying 11 thick (>1 m) pumiceous units derived from sustained explosive eruptions of Centre Hills from ~0.8–0.4 Ma. Over 10 other, less well- exposed pumiceous units have also been identified. The pumice-rich units are interbedded with andesite lava breccias derived from effusive, dome-forming eruptions of Centre Hills. The stratigraphy indicates that large (up to magnitude 5) explosive eruptions occurred throughout the history of Centre Hills, alongside effusive activity. This behaviour at Centre Hills contrasts with

Soufrière Hills, where deposits from sustained explosive eruptions are much less common and restricted to early stages of activity at the volcano, from ~175–130 ka. Subsequent eruptions at Soufriere Hills have been dominated by andesitic effusive eruptions. The bulk composition, petrography and mineral chemistry of volcanic rocks from Centre Hills and Soufrière Hills are similar throughout the history of both volcanoes, except for occasional, transient departures to different magma compositions, which mark shifts in vent location or dominant eruption style. For example, the final recorded eruption of Centre Hills, before the initiation of activity at Soufrière Hills, was more silicic than any other identified eruption on Montserrat; and the basaltic South Soufrière Hills episode marked the transition to the current stage of predominantly effusive Soufrière Hills activity. The compositional stability observed throughout the history of Centre Hills and Soufrière Hills suggests that a predominance towards effusive or explosive eruption styles is not driven by major compositional shifts of magma, but may reflect local changes in long-term magma storage conditions that characterise individual episodes (on $10^5$ year timescales) of volcanism on Montserrat.

## 1. Introduction

Individual volcanoes commonly exhibit different styles of eruptive behaviour through time, characterised by shifts in eruption style, frequency or composition (e.g., Druitt et al., 1989; Bacon and Lanphere, 2006; Singer et al., 2008; Germa et al., 2011), and potentially reflecting changes in magma genesis, processing and storage in the underlying plumbing system (e.g., Humphreys et al., 2006; Brown et al., 2014). Reconstructing long-timescale ($10^3$–$10^5$ year) patterns in volcanic behaviour can provide insights into the physical and chemical parametres that govern eruptive styles at a volcano, and how the processes driving volcanism may vary during the development of an individual volcanic system.

The island of Montserrat, in the Lesser Antilles island arc, comprises three main volcanic centres and has been a site of active subaerial volcanism since at least 2.6 Ma. The most recent eruption of Soufrière Hills, from 1995 to 2010, involved the extrusion of andesitic lava domes, with periodic partial dome collapse and vulcanian explosions (Druitt and Kokelaar 2002; Wadge et al., 2014). This eruption and the underlying Soufrière Hills magma system have been extensively studied (e.g., Barclay et al., 1998; Edmonds et al., 2001; Devine et al., 2003; Humphreys et al., 2009), but relatively little is known about the earlier history of volcanism on Montserrat. $^{40}Ar/^{39}Ar$ dating (Harford et al., 2002; Brown and Davidson 2008) and stratigraphic studies (Rea et al., 1975; Baker et al., 1985; Wadge and Isaacs 1988; Roobol and Smith 1998; Smith 2007) indicate andesitic subaerial activity at Soufrière Hills since ~290 ka, is dominated by effusive eruptions, and interrupted by a brief interlude of basaltic volcanism at the South Soufriere Hills at ~130 ka (Harford et al., 2002; Cassidy et al., 2015). Offshore studies may suggest volcanism occurred earlier at Soufrière Hills (Coussens et al., 2016a, 2016b; Jutzeler et al., 2016). Prior to this, current dates for subaerial activity at Centre Hills span the interval 0.95–0.55 Ma, and 2.6–1.2 Ma for Silver Hills, the oldest volcanic centre on Montserrat (Figure 1). Volcaniclastic deposits within the offshore sedimentary stratigraphy (e.g., Watt et al., 2012; Trofimovs et al., 2013) provide a more complete record of volcanic activity at Montserrat (Coussens et al., 2016a, 2016b), and suggest a more continuous level of volcanism than indicated by dated subaerial units (which imply gaps on $10^4$-year timescales between activity at the individual volcanic centres). However, many of these offshore deposits are mixed volcaniclastic turbidites, potentially derived from a range of primary and secondary volcanic processes (e.g. Trofimovs et al., 2013; Cassidy et al., 2014a). Eruption style is thus difficult to determine from the marine stratigraphy, but is more easily assessed from proximal subaerial exposures of volcaniclastic deposits.

This paper provides the first description of the onshore stratigraphy in the central part of Montserrat, based mainly on exposures along the east and west coasts. These deposits are mostly of Centre-Hills age, and we compare the stratigraphic record obtained with that of Soufrière Hills. By producing a record of volcanism on Montserrat since ~1 Ma, we aim to document the timing of major phases of activity, to determine how the style of volcanism has varied over this period, and to assess whether this variation followed consistent trends during the development of the Centre Hills and Soufrière Hills magmatic systems.

## 2. Methods

Past stratigraphic studies (e.g., Roobol and Smith, 1998; Harford et al., 2002) show that individual eruptions on Montserrat have involved a range of processes, including effusive activity, partial lava-dome collapses (generating pyroclastic density currents; PDCs), short-lived vulcanian explosions, and sustained explosive eruptions. The latter type of activity produces relatively widespread, pumice-rich tephra-fall and PDC-derived deposits, forming extensive stratigraphic horizons that can be correlated based on physical or chemical characteristics (e.g., Lowe 2011). These widespread pyroclastic deposits define discrete episodes of volcanic activity and can therefore be used to reconstruct local stratigraphic frameworks. To investigate the volcanic stratigraphy exposed in the central part of Montserrat we therefore focus principally on pumice-rich units, which have more potential for inter-site correlation and ultimately for correlating between subaerial exposures and the marine sedimentary record.

## 2.1 Fieldwork

Fieldwork was conducted in February 2013, investigating exposures in road cuttings and coastal cliffs throughout the central region of Montserrat (Figure 1). Areas affected by the 1995-2010 eruption of Soufrière Hills, as well as the northernmost part of the island, where the oldest rocks on Montserrat are exposed around the deeply eroded Silver Hills volcano, were excluded from this study. The study area is therefore broadly centred around the Centre Hills volcano, which consists of three steep-sided hills that merge together to form the central peak of Katy Hill, where exposed blocky lavas are likely to represent the approximate site of the main Centre Hills vent (Harford et al., 2002). Centre Hills is cut by several steep valleys. This part of the island is densely forested, and inland exposure is poor and limited to a few road cuttings. The coastal cliffs provide much more extensive exposures, typically ranging from 10 m to 50 m in height on the west coast, and 30 m to 100 m on the east coast (Figure 1).

The exposures studied here preserve proximal facies, with depositional patterns controlled by local topography, and widespread erosion affecting deposit preservation. Exposures are often laterally discontinuous, hindering stratigraphic correlation between sites. Pumice-rich pyroclastic deposits provided the most distinct units (in terms of physical appearance and sedimentological characteristics) and facilitate the correlation between sites across the island. Field correlation of pyroclastic deposits thus forms the basis of the stratigraphy presented here. Bulk and glass chemical analyses (Section 2.2) were used to resolve ambiguities in the field-based stratigraphy and to test correlations.

Many of the pyroclastic deposits studied here are internally complex, but have been grouped together as a single eruptive unit where they appear as a continuous stratigraphic sequence dominated by juvenile pyroclastic material of similar characteristics (e.g. colour, phenocryst assemblage). It is inferred that each of these units were formed during one eruption, albeit with potential variations in eruption style.

Approximately 15 km of coastal exposures and 8 road cuttings were logged around Montserrat to record the physical appearance, structure, mineralogical and sedimentological characteristics of individual deposits. Pumiceous deposits were sampled for chemical analysis, and maximum lithic and pumice clast sizes were determined by measuring the mean of the orthogonal axes of the three largest clasts found within a 10-metre length outcrop. Deposits were described using the terminology outlined by White and Houghton (2006), and PDC deposits identified using criteria outlined in Branney and Kokelaar (2002). In some sections, weathering (discolouration and clay alteration) affected the appearance of exposures, and because we cannot be certain if outcrops preserve original textures, we do not distinguish between consolidated and unconsolidated units (ash is thus used to describe grain-size (<2 mm) but not outcrop lithification).

## 2.2 Whole rock Chemistry

Lapilli-sized pumice clasts were collected from most of the identified pumiceous units, with some additional sampling of lithic clasts and ash deposits. Fresh clasts (i.e. showing no visible evidence of alteration or discolouration; this was possible for all pumiceous units except the Angry Bird pumice) were selected for bulk chemical analysis of major (XRF; Philips Magix Pro wavelength- dispersive XRF at the National Oceanography Centre, Southampton) and trace (XRF and ICP-MS; VG Plasmaquad PQ2 þ at the National Oceanography Centre, Southampton) elements. Samples were rinsed, dried and crushed before being ground to a fine powder using a tungsten carbide mill. Powder pellets and glass beads were prepared for XRF analysis, using the JA-1, BCR1, and BE-N standards. For ICP-MS, 0.05g of powder was dissolved in 3% $HNO_3$ and 3% HF, and then dried and re-dissolved with ~5 g HCl topped up to 10 g with MilliQ Water. 0.5 ml of this solution was then extracted and dried overnight. The residue was then re-dissolved, and made up to a 10 g solution with 3% $HNO_3$ solution with 5 ppm of indium and rhenium to achieve a dilution factor of 4000. Precision for all elements was generally better than 2%, except for Ni and Cs where precision was better than 6% RSD (see Supplementary Data).

## 2.3 Mineral and glass compositions

Mineral and glass chemistry were analysed in juvenile clasts from all pumiceous units. For mineral chemistry a Leo 1450VP scanning electron microscope (SEM) with an Oxford Instruments X-Act 10 $mm^2$ silicone drift detector and energy dispersive spectroscopy was used at the National Oceanography Centre, Southampton. Beam current was 10 nA with an analysis time of 180 seconds. Haematite and clinopyroxene standards were used to check for instrument drift and calibration. All analyses presented here have been normalised to 100 wt.% anhydrous compositions. Standard deviation of results is generally <0.4 wt.% (raw data are provided in Supplementary Tables).

Glass chemistry was analysed using a Cameca SX100 microprobe at the School of Earth Sciences, University of Bristol. A beam current of 4 nA was used with a beam diametre of 5 µm and an analysis time of 180 seconds. Each sample was analysed multiple times. Any totals of <95 wt.% were discarded. Pumice clasts from several separate locations were analysed to test stratigraphic correlations (raw data are provided in Supplementary Tables).

## 2.4 $^{40}Ar/^{39}Ar$ dating

A small number of pumiceous units were selected for $^{40}Ar/^{39}Ar$ dating. The glassy groundmass of these pumice clasts was unsuitable for dating, and plagioclase phenocrysts were therefore picked out for dating. Samples were crushed using a jaw crusher and then wet sieved and left to dry overnight. Plagioclase crystals were separated from sieved fractions of 125-250 µm and 250-500 µm using a model LB-1 Frantz magnetic separator.

Samples and neutron flux monitors were placed in copper foil packets and stacked in quartz tubes. The relative positions of wells in the discs were precisely measured for later reconstruction of neutron flux gradients. The sample package was irradiated for 2.0 hours in the Oregon State University reactor, Cd-shielded facility. Alder Creek sanidine (1.2056±0.0019 (1□ Ma, Renne et al. 2011) was used to monitor $^{39}Ar$ production and establish neutron flux values (J) for the samples.

Gas was extracted from samples using a mid-infrared (10.6 µm) $CO_2$ laser. Liberated argon was then purified of active gases (e.g., $CO_2$, $H_2O$, $H_2$, $N_2$, $CH_4$) using three Zr-Ti-Al getters; one at 16°C and two at 400°C. Data were collected on a GVi instruments ARGUS

V multi-collector mass spectrometer using a variable sensitivity faraday collector array in static collection (non-peak hopping) mode (Mark et alk 2009; Sparks et al. 2008). Time-intensity data are regressed to $t_0$ with second-order polynomial fits to the data. Mass discrimination was monitored by comparison to running-average values of an air standard. The average total system blank for laser extractions, measured between each sample run, was $2\times10^{-15}$ mol $^{40}$Ar, $3\times10^{-17}$ mol $^{39}$Ar, $3\times10^{-18}$ mol $^{36}$Ar.

All data are blank, interference and mass discrimination corrected using the Massspec software package (authored by Al Deino, BGC). Plateau acceptance criteria are that the plateau consists of at least three contiguous steps and the scatter between the ages of the steps is low, i.e., MSWD close to 1, and the fraction of $^{39}$Ar released for these steps is ≥50%. Isochrons are calculated using only the plateau steps to confirm that the composition of the trapped component. A plateau age is accepted if it is concordant at the 2σ level with the isochron age, has a trapped component indistinguishable from air (298.56±0.31, 1σ) at the 2σ level and meets the other criteria listed above.

The Ar-Ar dates obtained in this study have relatively large errors, with 2 σ errors of 0.11 to 0.21 Ma, due to the low K content of Montserrat's eruptive products. It is also important to note that results may be biased towards older ages due to xenocrystal plagioclase (cf. Harford et al., 2002).

## 3. Results

### 3.1 Volcanic stratigraphy

The stratigraphy of volcanic deposits exposed in central Montserrat is summarised in this section. The stratigraphy has been developed primarily from field relationships, with some refinements based on bulk or glass chemistry.

Exposures throughout the study area comprise a mixture of pumice-rich deposits (with individual thicknesses of up to 16 m, but generally less) interbedded with generally thicker deposits of dense andesite lava breccias (often >10 m in thickness) (Figures 2 to 4). Pumiceous units are frequently lenticular and laterally discontinuous, with eroded upper surfaces overlain by lithic-rich deposits. As such, the full primary thickness of pumiceous units is not always preserved. Andesite lava breccias have similar physical characteristics throughout the area, being dominated by poorly sorted, angular dense grey andesite blocks. Individual deposits have lateral extents of tens to hundreds of metres, with poorly developed grading or internal bedding. The lateral variation and similar appearance of these andesite lava units throughout the area hinders their direct correlation between sites. The andesite lava breccias may represent primary or secondary deposits associated with lava-dome forming eruptions, as well as mass wasting and alluvial processes. Although they cannot be correlated directly, packages of lithic units can be defined by their bounding pumiceous deposits, which are more easily correlated between sites due to their more distinctive appearance and widespread nature (particularly tephra fall deposit components).

Pumiceous units to the northeast and southwest of Centre Hills can be traced laterally in cliff exposures for several hundred metres. To the west, northwest and southeast, more extensive localised erosion has produced discontinuous deposits, typically forming channels filled with andesite lava breccias erosively truncating pyroclastic units. In total, twenty four individual pumice-rich units have been identified based on their physical appearance, stratigraphic order and chemistry. Many of these units are poorly exposed and only recognised from a single site (these units are often relatively thin (<1 m). The poor

ACCEPTED MANUSCRIPT

preservation of several units suggests that our stratigraphy is likely to be incomplete, with the products of smaller explosive eruptions having little or no representation in subaerial exposures. Twelve of the identified pumiceous units are more laterally extensive or thicker, and have been investigated in more detail. Many of these have been correlated across multiple sites (Figures 2 and 3) and used to produce a local stratigraphic framework. A brief description of each of these units is given below, in approximate stratigraphic order, with more detailed lithofacies descriptions in Table 1.

3.1.1 Exposures west of Centre Hills

Cliff exposures along the west coast of Montserrat are more extensive than exposures on the east coast, and preserve a larger number of pyroclastic deposits, even though the cliffs are generally higher on the east coast. We therefore describe units exposed west of Centre Hills first. In general, the thickest pumiceous deposits are found east of Katy Hill (Figure 1) and have a thinning pattern that is consistent with a provenance from Centre Hills. This is less clear for the Bransby Point and Garibaldi Hill pumices, which could potentially be derived from a more southerly vent site. The wide submarine shelf around Bransby Point (Figure 1) suggests that this southern part of the island is older than Soufrière Hills (which has a very narrow submarine shelf), and it is possible that older volcanic vents in this region are now buried beneath younger volcanic rocks. However, the small number of field sites makes it difficult to identify vent sites precisely for any of these units.

Only one unit, the Old Road Bay pumice, was found both east and west of Centre Hills. The relative age of east- and west-coast deposits above and below this tie point is thus uncertain, but has been investigated by $^{40}Ar/^{39}Ar$ dating (Section 3.3).

To the southwest of Centre Hills, five extensive pumice-rich units (Old Road Bay pumice, Garibaldi Hill pumice, Bransby Point pumice, Old Road Bay tuff, and Foxes Bay pumice) overlie the less well exposed South Lime Kiln Bay pumice. To the northwest of Centre Hills, three stratigraphically younger units are well exposed (the Bunkum Bay pumice, Woodlands Bay pumice, and the Attic pumice).

*South Lime Kiln Bay pumice*

The South Lime Kiln Bay pumice crops out within a faulted block at Lime Kiln Bay (southwest of Katy Hill) that exposes relatively older strata. In this area the exposure is a pumice-dominated medium (4-16 mm) -lapilli tuff, which is up to 7 m thick and divided into three units (Table 1). Decimetre- to- metre-scale beds of variably- sorted pumice lapilli (90% pumice) are interbedded with thin medium- to- coarse- grained ash beds and lithic-rich intervals. The proportion of lithic clasts increases in the uppermost part of the unit.

*Interpretation*

The full unit is interpreted as a sequence of tephra fall and high-concentration PDC deposits.

*Old Road Bay pumice*

The Old Road Bay pumice has been identified across several sites and is the only unit identified in coastal exposures both east and west of Centre Hills (Figures 2 and 3). The unit is one of the stratigraphically oldest deposits on the west coast. It comprises a series of pumice-rich (up to 80 vol.%) lapilli-tuff deposits with lenses of well-sorted pumice lapilli and discontinuous ash-rich horizons. The unit has a total thickness of up to 6 m comprising three main units (Table 1). The lower units preserve occasional cross stratification, with the middle unit comprising banded beds of ash and lapilli, with accretionary lapilli in places. The uppermost unit comprises the bulk of the deposit and is a massive, poorly-sorted mixture of pumice and lithic clasts. Pumice clasts throughout the deposit are buff coloured and the cement weathers to a distinctive pink-orange colour.

*Interpretation*
The lower, banded units are interpreted as the reworked (i.e. partially rounded) products of fall deposits from repetitive explosive activity and/or low concentration PDC deposits. The thick, poorly sorted, uppermost unit is interpreted as the product of a high-concentration PDC.

*Garibaldi Hill pumice*
The Garibaldi Hill pumice is well exposed around Garibaldi Hill, where it has been locally uplifted and tilted. The deposit has a total thickness of up to 5.5 m and is formed of a pumice-rich, coarse (16-64 mm)-lapilli- tuff that crops out to the south west of Centre Hills. The lower unit comprises of poorly- sorted lapilli-tuff, capped by an upper massive unit of well-sorted angular pumice lapilli (95 vol.% pumice) (Table 1). The unit thins northwards into a laminated grey tuff with a distinctive pink tuff top.

*Interpretation*
The lower unit of poorly sorted lapilli tuff is interpreted as a high-concentration PDC deposit, the well sorted upper unit interpreted as a fall deposit (Table 1).

*Bransby Point pumice*
The Bransby Point pumice is laterally continuous over a distance of 3 km in the south west part of Montserrat at Bransby Point and Foxes bay, thinning northwards. It has a distinctive grey and pink colour, and can be divided into two units of similar thickness (2 m total). Both units contain well- sorted, angular pumice lapilli. The lower bed is white to grey in colour, with weak internal stratification developing on a decimetre scale. It is capped by a thin (<10 cm) pink ash. The upper unit is more massive, containing pink pumice clasts, with discontinuous 1-cm thick ash horizons, capped by a 5 cm ash deposit.

*Interpretation*
These deposits are interpreted as fall deposits from a sustained explosive eruption.

*Old Road Bay tuff*
This unit forms a distinctive ash-rich marker bed that can be traced widely along the west coast of Montserrat, comprising of two sub units that have a combined thickness of up to 1 m (Table 1). The lower bed is a well-sorted laminated tuff that has faint decimetre-scale bedding, grey at the upper and lower margins and yellow in the centre. The upper bed has a more variable thickness and is coarser. The upper bed has centimetre-scale bedding that comprises yellow ash beds and fine (2-4 mm)-lapilli beds that are a single clast thick.

*Interpretation*
The lateral continuity and sorting of the lower bed suggests an origin as a fall deposit, while the upper part may result from a low-concentration PDC associated with an unsteady explosive eruption.

*Foxes pumice*

The Foxes pumice is poorly exposed at a single site on the south west coast of Montserrat, but forms a thick (3.2 m), well-sorted pumice-rich deposit (Table 1). The lowermost part is a well-sorted, pink medium (0.25-0.5 mm)-ash deposit, with faint lamination, overlain by a massive 3 m thick well-sorted angular pumice (>90 vol.%) lapilli deposit, with poorly developed decimetre-scale bedding.

*Interpretation*

The unit is interpreted as a fall deposit from a large sustained explosive eruption.

*Bunkum Bay pumice*

The Bunkum Bay pumice crops out only at Bunkum Bay, forming a series of overlapping channels of alternating orange-brown lapilli-tuff and tuff beds (Figure 4c), exceeding 3 m in thickness. The unit comprises poorly-sorted ash-rich beds with variable proportions of pumice and lithic clasts, including horizons rich in accretionary lapilli (Table 1). Some beds show low angle bedding and reverse grading. The deposit is overlain by a massive 7 m thick polymict deposit, which was inaccessible.

*Interpretation*

The variable composition and structure suggests that the deposit may be the product of a sequence of unsteady high-concentration pyroclastic density currents. The overlying massive unit may reflect reworking (e.g. lahar deposits) of deposits from the same eruption.

*Woodlands Bay pumice*

The Woodlands Bay pumice is one of the coarsest and thickest pumiceous deposits exposed on Montserrat. The unit has a total thickness of up to 16 m and crops out at several locations on the west and north west of Montserrat. The lower parts of the unit comprise variably sorted beds on metre- to- decimetre-scales, dominated by buff-coloured pumice, with some lithic rich horizons and cross-bedded lenses. This is overlain by a thick central sequence of pumice-rich (70-90 vol.%) moderately- to well-sorted lapilli beds on metre- to decimetre-scales, with a mean pumice clast size of 2-4 cm and maximum size of 11 cm. These coarse lapilli beds are interspersed with more ash-rich (< 40 vol.% of pumice) lapilli beds. This is overlain by a thick (>5m) upper sequence of coarser (mean pumice clast size of 4.5 cm; maximum size of 18 cm) decimetre bedded lapilli beds that are moderately- to- well- sorted.

*Interpretation*

The lower most units are interpreted as the product of high-concentration PDCs (Table 1) due to their lateral variability, compositional variation, and development of cross bedding. The central part of the unit is interpreted as tephra fall deposits interleaved with pumice-rich PDC deposits. Some local horizons within this central unit may have also been reworked.

The upper most part of the unit is interpreted as fall deposits derived from sustained explosive activity. Variations in grain size through the unit suggest that there were slight fluctuations in explosive intensity.

*Attic pumice*

The Attic pumice is the youngest of the pumiceous deposits studied here, and is best exposed in road cuttings on the west side of Montserrat. The unit forms a 3 m thick sequence of white, metre-scale fine-lapilli tuffs, with abundant ash-coated pelletal pumice grains (Figure 4e). The lower part of this unit has planar laminations in places, while the upper section is cross-bedded, coarser and more poorly- sorted, with some relatively larger lithic clasts. It overlies a thicker (up to 3 m) bed of medium-coarse lapilli-tuff that is poorly exposed. This unit has fewer pelletal grains, particularly near the base, and contains lenses of coarse pumice lapilli with some bedding structures (Table 1).

*Interpretation*
The entire sequence is interpreted as the product of wet low- to moderate-concentration PDCs, given the abundance accreationary lapilli and pelletal grains, and the development of flow structures (e.g. cross bedding, low angled bedding).

3.1.2 Exposures east of Centre Hills
Four pumiceous units are well exposed on cliff sections east of Centre Hills (there are few road cuttings in this area). One of these, the Old Road Bay pumice, also occurs west of Centre Hills and is described above. The Old Road Bay pumice lies above the Angry Bird pumice, and at a similar stratigraphic level to the Bramble pumice (their relative age cannot be deduced from field exposures). Above these, the youngest unit on the east coast is the Statue Rock pumice.

*Angry Bird pumice*
The Angry Bird pumice crops out only on the east coast of Montserrat near Bramble Airport and around Statue Rock. It lies stratigraphically below the Old Road Bay pumice. The unit comprises up to four massive pumice-rich lapilli deposits, which are truncated by massive lithic-rich channel-fill deposits. Pumice clasts are 1-2 cm in diametre, angular- to-sub-angular with a flattened shape, and are altered to soft clays (Table 1). The beds have a pink ash matrix (10 vol.%) and infrequent lithic clasts (1 cm; 5 vol.%). Beds thin northwards, and are laterally continuous over several hundred metres. The lowermost pumice bed directly overlies a glassy porphyritic (35 vol.% plagioclase; 15 vol.% pyroxene) lava flow at the Bramble Airport exposures.

*Interpretation*
The pumice-rich beds are interpreted as tephra fall deposits, with the lithic sequences perhaps reflecting mass-wasting deposits derived from associated effusive activity.

*Bramble pumice*
The Bramble pumice is poorly preserved on the east coast as thin (cm-thick; ~10 m lateral extent) bands or lenses within a 12 m thick sequence of massive andesite lava breccias (Table 1). The unit also contains a bed of distinctive slab-shaped rip-up clasts of laminated ash.

*Interpretation*
The pumiceous component of the unit appears to be largely reworked, and it is difficult to assess the characteristics of the primary eruption deposit.

*Statue Rock pumice*
The Statue Rock pumice crops out on the east coast at Statue Rock and can be traced along the cliff section for ~1 km. The unit is a poorly sorted lapilli-tuff with a matrix of yellow coarse crystalline ash, with localised lenses of andesite lava breccia and pumice lapilli. The overall unit displays low angle cross bedding and has a laterally variable thickness of ~10 m (Table 1).

*Interpretation*
We interpret the unit as partially reworked deposits of high-concentration PDCs.

3.2 Chemistry and petrography
The pyroclastic units described above were defined using field relationships. We have analysed the bulk pumice chemistry of each of these units, and in some cases have used additional glass and mineral analyses to test field correlations. We identified no evidence of compositional heterogeneity in the juvenile products of any of the deposits studied here (i.e. changes in the colour, mineral content and phase assemblage of pumice clasts), suggesting that the magma erupting in each event was compositionally homogeneous. This is supported by glass analyses from individual units sampled across several sites, which form distinct clusters in their major-element chemistry. The bulk chemistry of all pumiceous units analysed here is broadly similar, but there is sufficient compositional variation to discriminate between individual units.

3.2.1 Major element chemistry
The bulk pumice silica composition (Table 2) lies between 58 and 63 wt.% for all the units studied here, defining them as andesites, except for the Attic pumice (the youngest unit), which is slightly more silicic (65.4 wt.% $SiO_2$; dacite), and the Angry Bird pumice (52.3 wt.% $SiO_2$; basaltic andesite) (Figure 5). The latter is the stratigraphically oldest deposit here (alongside the South Lime Kiln bay pumice; their relative age cannot be deduced), and is also the only deposit where the pumice clasts were extensively altered to clay minerals. This alteration may have affected its bulk chemistry, although its overall major element contents are not atypical for basaltic andesites, and lie on consistent fractionation trends with the andesitic units. Notwithstanding the potential effects of alteration, the Angry Bird pumice therefore appears to be distinctively more mafic than the other units studied here (Figure 5). Analyses of seven additional un-named pumiceous units (Table 2) also fall within the andesitic compositional range above (one sample is very slightly more mafic, at 56.8 wt% $SiO_2$), suggesting that nearly all the large explosive eruptions from Montserrat throughout the studied stratigraphic period erupted andesitic products.

All the samples lie on tholeiitic and medium K-series trends (<1 wt.% $K_2O$), forming a linear compositional array where the observed chemical variation can be attributed to fractional crystallisation processes (Figure 5). These compositions are similar to previously reported data for lavas from Centre Hills and Silver Hills (56–64 wt.% $SiO_2$) (Cassidy et al., 2012; Harford et al., 2002), although both the Angry Bird and Attic pumices fall outside this previously recognised compositional range. When all the units are placed in stratigraphic order (Figure 6), there is no apparent temporal variation in major element compositions except for a general trend towards more potassic compositions in younger units (the Statue Rock pumice lies off this trend). The Attic pumice is the most chemically evolved unit studied and is easily discriminated from the other units by its bulk composition. The other units cannot easily be distinguished on the basis of major element bulk composition.

3.2.2 Trace element chemistry
Whole-rock trace element compositions of pumices (Table 3) show more inter-unit variation than major element compositions and can be used to distinguish between units. For example, Nd and Y compositions (Figure 7) cluster tightly for individual deposits, defining discrete compositional ranges that can be used for inter-site correlation. Plotting

the units in stratigraphic order (Figure 6) indicates long-term trends towards relative HREE depletion in the younger units (i.e. higher La/Lu ratios) and enrichment in high field-strength elements such as Th. The more evolved Attic pumice again has compositions (e.g. high Ba contents) that distinguish it from the other units. The low Ba content of the Angry Bird pumice may reflect its extensive alteration, resulting in low concentrations of mobile elements.

Lavas from Centre and Silver Hills have a relatively lower Ba/La ratio compared to the Soufrière-South Soufrière Hills volcanic complex (Cassidy et al., 2012). This relationship can be used to test our stratigraphic inference, based on the general thickening of pyroclastic deposits within the central part of Montserrat, that most of the units identified here are derived from Centre Hills. All the samples analysed here (all named units except Bransby point, and nine additional un-named units; Table 3) form a clustered group with slightly lower Ba/La than Soufrière Hills (Figure 8), overlapping with previous Centre/Silver Hills data, but displaced slightly to higher Th/La values. This supports an origin from Centre or Silver Hills for these units.

3.2.3 Mineral and glass chemistry

Pumice clasts from all the studied units are highly porphyritic (similar to andesitic lavas from Montserrat), with phenocryst contents ranging from 20 to 50 vol.%. The typical phenocryst assemblage in all the studied units is plagioclase + hypersthenes + Fe-Ti oxides ± augite/low Fe diopside ± quartz. The Attic pumice (the most silicic and youngest unit) is also mineralogically distinctive, with a phenocryst assemblage of hypersthene + hornblende + plagioclase + quartz. With the exception of the Attic pumice, the absence of phenocryst hornblende distinguishes the studied units from the magmas erupting at Soufrière Hills since ~130 ka, which have hornblende as a phenocryst phase (cf. Harford et al., 2002; Cassidy et al., 2015).

Pyroxene phenocrysts showed no significant compositional zoning within the analysed units. Orthopyroxene phenocrysts are Fe-rich hypersthenes with core compositions of $Fs_{33-38}En_{59-65}Wo_{1-5}$ (n=30) and very similar rim compositions of $Fs_{34-38}En_{60-64}Wo_{1-2}$ (n=29) (Figure 9). Clinopyroxene phenocrysts are mostly low-Fe diopside or high-Ca augite with core compositions of $Fs_{15-18}En_{39-41}Wo_{43-44}$ (n=32) and rim compositions of $Fs_{15-18}En_{38-41}Wo_{43-47}$ (n=27) (Figure 9). Plagioclase phenocrysts are varied and complex, exhibiting oscillatory, normal and reverse zoning spanning a range of relatively anorthitic compositions (core compositions of $An_{77-91}$ (n=34) and rim compositions of $An_{79-94}$ (n=28). The amphibole phenocrysts in the Attic pumice are classified as magnesio-hornblende based on their aluminium content.

Orthopyroxene crystals show trace variations in chemistry between the major stratigraphic units from Centre Hills (Figure 9). Subtle variations in the Fe and Al content in the rims of orthopyroxene phenocrysts occur between different units, and can distinguish units with very similar bulk chemical compositions (e.g. the Attic and Bramble pumices; Figure 9). Orthopyroxene rim chemistry may thus be a further characteristic (alongside bulk trace element and glass compositions) that has potential for deposit correlation, particularly when tying these subaerial deposits with the offshore stratigraphy.

Groundmass glass chemistry is widely used to characterise tephra fall deposits for chemical correlation (Lowe 2011), and was measured by EPMA on samples with no visible alteration (the Angry Bird pumice was therefore not analysed, and the Bunkum Bay deposit was also excluded based on the scatter shown in its $K_2O$ glass contents). Samples typically formed tightly clustered $K_2O$ compositions, suggesting that glass chemistry was invariant during individual eruptions. All units have broadly similar, rhyolitic glass compositions (70-80 wt.% $SiO_2$), with small variations in $TiO_2$, $K_2O$ and MgO (Figure 10) that define distinct field for a few units (Bransby Point, Foxes and Attic pumices), but largely overlapping fields for all other units. The Bransby Point pumice is distinctive in having a high glass $K_2O$ content (~2.5 wt.%).

From the small amount of data collected here, pre-eruptive magma storage temperatures can be estimated using amphibole, orthopyroxene-liquid, clinopyroxene-liquid, and plagioclase-liquid geothermobarometry. This is not intended to be a comprehensive survey, but indicates the broad temperature ranges of magmas feeding the eruptions studied here and can be used to compare with data from Soufrière Hills. Analyses are based on phenocryst and co-existing glass compositions (Ridolfi et al., 2010; Putirka et al., 2003, 2005, 2008). Different geothermometres have been used depending on the phases present, and the results of different methods cannot necessarily be directly compared. For the Attic pumice, amphibole geothermometry indicates temperatures of 812–852°C (n=10). Higher temperatures are derived from an orthopyroxene-melt geothermometre for the South Lime Kiln Bay pumice (947–1080°C; n=13) (note that orthopyroxene rims could not be used for any other units, because they did not pass a melt equilibrium test based on $Kd_{(Fe\text{-}Mg)}$). Analyses from other units (see Supplementary Data tables) using a clinopyroxene-melt geothermometre (conducted on rims that pass the $Kd_{(Fe\text{-}Mg)}$ equilibrium test) indicate a slightly cooler but similarly broad temperature range of 894–1022°C (n=7) (using pressure independent equations from Putirka et al. (1996). Slightly higher temperatures are produced by plagioclase-melt geothermometry (1003–1032°C; n=17) (plagioclase rims only, passing a $Kd_{(Ab\text{-}An)}$ equilibrium test) (Putirka et al., 2005).

### 3.3 Ages

Both stratigraphic thickening patterns and trace element chemistry suggest that the units studied here are derived from Centre Hills, although it is possible that some of the basal stratigraphic units (South Lime Kiln Bay and Angry Bird pumices) originate from Silver Hills (trace element chemistry cannot distinguish the two sources), or that some of south-western units (Bransby Point and Garibaldi Hill pumices), based on tephra fall deposit distribution, could originate from a slightly more southerly vent site. The age of the stratigraphy studied here has been investigated further by $^{40}Ar/^{39}Ar$ dating, providing direct dates for six units (Figure 11). Previous $^{40}Ar/^{39}Ar$ dates for Centre Hills span 0.95–0.55 Ma (Harford et al., 2002), and 2.6–1.2 Ma for Silver Hills (Harford et al., 2002; Brown and Davidson, 2008).

The stratigraphically oldest units identified here are the Angry Bird and South Lime Kiln Bay pumices. The Angry Bird pumice was too altered to be suitable for dating, but $^{40}Ar/^{39}Ar$ analysis for the South Lime Kiln Bay pumice, using plagioclase phenocrysts, indicates an age of 1.31 ± 0.21 Ma (Figure 11; all errors quoted at 2σ level). This overlaps with the youngest end of the known period of activity at Silver Hills (Harford et al., 2002), which is thus the likely source for this unit. Unlike the South Lime Kiln Bay pumice, which occurred in an isolated faulted block, the Angry Bird pumice can be related stratigraphically to the rest of the units studied here, because it lies just a few metres below the Old Road Bay pumice (Figure 2). The Old Road Bay pumice is exposed on both the east and west coasts and has a thickening pattern that suggests an origin from Centre Hills. This is confirmed by an $^{40}Ar/^{39}Ar$ age of 0.70 ± 0.14 Ma, which overlaps with the central stage of previously-dated Centre Hills volcanism (Harford et al., 2002). Given this age, we infer that the underlying Angry Bird pumice is also of Centre-Hills age.

Stratigraphically above the Old Road Bay pumice lies the Garibaldi Hill and Bransby Point pumices. The latter has an $^{40}Ar/^{39}Ar$ age of 0.79 ± 0.17 Ma. Although this is older than the Old Road Bay pumice date, the dates are stratigraphically consistent if the relatively large dating errors are taken into account. The similar ages obtained for the Old Road Bay and Bransby Point pumices suggests that this stage of Centre Hills volcanism (~0.8-0.6 Ma) was characterised by several large explosive eruptions (Angry Bird, Old Road Bay, Bramble, Garibaldi Hill and Bransby Point pumices, as well as a number of un-named interbedded deposits, and followed by the stratigraphically younger but undated Old Road Bay tuff, Statue Rock pumice and Foxes pumice).

The Bunkum Bay, Woodlands Bay and Attic pumices crop out extensively west and northwest of Centre Hills, and form a younger stratigraphic package. $^{40}Ar/^{39}Ar$ ages are 0.51 ± 0.11 Ma for the Bunkum Bay pumice, 0.59 ± 0.11 Ma for the Woodlands Bay pumice, and 0.48 ± 0.20 Ma for the Attic pumice. Within error, these ages are again consistent with stratigraphic order, and suggest that these three eruptions all originated from Centre Hills at ~0.5 Ma.

The distinct stratigraphic distribution of the three youngest units studied here (Bunkum Bay, Woodlands Bay and Attic pumices) suggests that they may represent a separate phase of volcanism at Centre Hills, but within the error of the $^{40}Ar/^{39}Ar$ dates there is no evidence of a significant pause in explosive volcanism at Centre Hills. The ages indicate that at least eleven explosive eruptions (or at least 22, taking into account un-named and uncorrelated deposits) originated from the Centre Hills volcano between ~0.8 and 0.4 Ma. These dates extend the period of Centre Hills volcanism to slightly younger ages, and reduce the apparent gap in subaerial volcanism before the oldest dated activity further south on Montserrat, at ~290 ka (Harford et al., 2002). Volcaniclastic deposits in submarine sedimentary sequences provide no evidence of prolonged pauses in volcanism at Montserrat (Coussens et al., 2016a).

### 3.4 Eruption Parametres

Partial isopachs have been constructed for tephra fall deposits (Table 1) that could be correlated across multiple sites, using maximum cumulative fall deposit thicknesses at each site (Figure 12). Constraints are generally poor due to limited subaerial exposure. Katy Hill was assumed as the vent location for all eruptions, and isopach shapes were estimated by fitting an ellipse to the available data. Isopach width is very poorly constrained for all deposits. The area of fitted isopachs was used to estimate a minimum fall deposit volume ($V_{min}$) using $V_{min} = 3.7\ A\ T$, where $A$ is isopach area (km$^2$) and $T$ is isopach thickness (m) (cf. Pyle, 1999). Calculated volumes range between 0.02 km$^3$ for the Attic pumice fall deposits and 0.43 km$^3$ for the Woodlands Bay fall deposits (Table 6) (these are not dense rock equivaent volumes). Legros et al. (2000) show that 70% of results are underestimated by at least a factor of two using this method, due to an absence of more distal depositional data. Several of these eruptions, as shown in Figure 12, also produced thick PDC deposits, with thicknesses exceeding 10 m in some cases at distances of several kilometres from the vent. The PDC deposit components of some of these eruptions may be greater in volume than the fall deposit components. Given these uncertainties, it seems likely that several of these eruptions had total tephra volumes of up to 0.5 km$^3$ and that some, such as the

Woodlands Bay pumice, were likely >1 $km^3$. Many of these eruptions thus had likely explosive eruption magnitudes of 4–5 (cf. Pyle, 2000).

**4. Discussion**

4.1 History of eruptive activity at Montserrat since 1 Ma

Based on the stratigraphy described above and on previous studies of Soufrière Hills (e.g., Roobol and Smith 1998; Harford et al., 2002; Smith et al., 2007) we have divided volcanic activity on Montserrat since 1 Ma into six episodes (Figure 13). Divisions between these episodes mark an absence of subaerial eruption related products, a change in eruptive vent, or a change in dominant eruptive style. The oldest unit identified here (South Lime Kiln Bay pumice) is not included in this summary because it could not be correlated with the rest of the stratigraphy and may originate from Silver Hills, or from the transitional period between the end of volcanic activity at Silver Hills and the onset of Centre Hills volcanism.

*Centre Hills Episode 1, >0.95 to ~ 0.6 Ma*

The oldest dated unit from Centre Hills is andesitic lava from an old lava-dome complex at the southern edge of Centre Hills, dated at 0.95 Ma (Harford et al., 2002). The major part of the stratigraphic sequence identified here forms a sequence of andesite lava breccias interbedded with pumiceous deposits from sustained explosive eruptions, erupted between ~0.8 and ~0.6 Ma. Deposits from this period are exposed northeast of Centre Hills and more extensively to the west and southwest of Centre Hills. There are no internal divisions that can be used to break this period up further. Because the base of these deposits (or a recognisable transition to Silver Hills deposits) is not exposed, we define the start of this first stage of Centre Hills volcanism at >0.95 Ma. The period included at least eight large explosive eruptions (and additional smaller, uncorrelated deposits), producing andesitic pumiceous deposits (with the exception of the Angry Bird basaltic andesite), and frequent effusive eruptions of compositionally similar andesitic lava (cf. Cassidy et al., 2012; Harford et al., 2002), whose collapse and erosion has generated extensive andesite lava breccias around the flanks of Centre Hills. The production of large explosive eruptions of evolved magma suggests a mature volcanic system. Active vent sites may have existed during this period to the south of the currently exposed Centre Hills rocks, given the wide eroded submarine shelf around Bransby Point (similar in width to the shelf around Centre Hills), and the distributional pattern of some tephra fall deposits (e.g. Bransby Point pumice).

*Centre Hills Episode 2, ~0.6 to ~0.4 Ma*

We have defined a second period of Centre Hills volcanism, based on our interpretation of the subaerial volcanic stratigraphy, where the three youngest pumiceous deposits (Bunkum Bay, Woodlands Bay and Attic pumices) are preserved as thick PDC deposits at sites lying slightly further north than the older units, and are well exposed west and northwest of Centre Hills. It is unclear from the dating if there was a prolonged ($10^5$ year) gap in explosive volcanism, but the distribution of these units suggests a more northerly vent, consistent with the current peak of the Centre Hills volcano at Katy Hill. As in Episode 1, this stage of volcanism involved sustained explosive eruptions, including the largest-volume explosive eruption deposit on Montserrat, the Woodlands Bay pumice, interspersed with effusive andesitic lava-dome forming eruptions.

Although the vent site may have moved to a more northerly position, both Episodes 1 and 2 at Centre Hills are characterised by effusive and large explosive eruptions throughout the history of the volcano, without any apparent transitions in dominant eruptive behaviour.

However, the youngest explosive eruption deposit, the Attic pumice, is distinctive. Its dacitic composition is more evolved than any other known volcanic rocks on Montserrat. The deposit forms the uppermost part of the stratigraphy west of Centre Hills, and is well exposed in road cuttings, where it lies immediately beneath the soil surface. It may potentially mark the final eruption of the Centre Hills volcano, and it is thus notable that this final event is compositionally distinctive, representing a maturation of the system towards more silica-rich compositions (and with stable amphibole in the phase assemblage, unlike any preceding Centre Hills eruptions).

*Soufrière Hills Episode 1, >0.3 to 0.175 Ma*

After the Attic pumice eruption, the next identified volcanism on Montserrat moved to the south, potentially distributed between effusive vents west of Soufrière Hills, around Garibaldi, Richmond and St Georges Hills (cf. Harford et al., 2002; Smith, 2007). It is uncertain if both the Soufrière and Centre Hills systems were active at the same time, but there is no prolonged gap in volcaniclastic deposition in the offshore stratigraphy at this time (Coussens et al., 2016a). Onshore, this period of volcanism on southern Montserrat is poorly exposed.

*Soufrière Hills Episode 2, 0.175 to 0.13 Ma*

Several lava domes from this period have been dated around Soufrière Hills, and the period is characterised by andesitic effusive volcanism and small- to moderate-sized explosive eruptions, preserved as pumiceous lapilli and tuff fall deposits up to 1.5 m thick and pumiceous surge deposits up to 2 m thick to the south of Soufrière Hills (Roobol and Smith, 1998; Smith, 2007). These deposits are the only evidence of sustained explosive eruptions from Soufrière Hills. The predominantly effusive andesitic behaviour of Soufrière Hills is thus in sharp contrast to the Centre Hills stratigraphy described here, which produced large explosive eruptions, alongside effusive activity, throughout its history.

*South Soufrière Hills Episode, ~0.13 Ma*

At ~0.13 Ma activity at Soufrière Hills shifted onto the south flank of the edifice, forming the South Soufrière Hills. This eruption produced basaltic scoria deposits with interleaving basaltic lava flows and andesite lava breccias, which are more mafic than any other volcanic rocks from Montserrat (Smith, 2007; Cassidy et al., 2014b, 2015).

*Soufrière Hills Episode 3, <112 ka*

Activity at Soufrière Hills returned to the central vent site after the South Soufrière Hills episode (Harford et al., 2002), and has been dominated by effusive eruptions of andesitic lava domes throughout this period, interspersed with short-lived vulcanian explosive pulses, and generating extensive andesite lava breccias around the volcano (Wadge and Isaacs, 1988; Roobol and Smith, 1998; Smith et al., 2007). Lavas erupted in this episode at hornblende-hypersthene andesites, in contrast with the clinopyroxene-hypersthene andesites that erupted in Episode 2 and throughout the history of Centre Hills (with the exception of the Attic pumice).

4.2 Comparison between Centre Hills and Soufrière Hills

The stratigraphy of the Soufrière Hills complex differs markedly from the stratigraphy of Centre Hills. Thick (>1 m) pumiceous deposits from sustained explosive eruptions are present throughout the stratigraphy of Centre Hills, but are confined to the early stages of activity at Soufrière Hills (Episode 2), and even at this time do not appear to have been as large or frequent (based on their limited preservation) as those from Centre Hills.

Rocks from Soufrière Hills Episode 3, and particularly those from the most recent eruption, have been far more extensively studied (e.g., Barclay et al., 1998; Edmonds et al., 2001; Devine et al., 2003; Humphreys et al., 2009) than older rocks from both Soufrière Hills and Centre Hills (e.g., Zellmer et al., 2003; Devine et al., 2003; Cassidy et al., 2015). However, available data suggests that, throughout the history of the two volcanoes, effusive eruptions have involved similar styles (dome extrusion and generation of associated andesite lava breccia deposits) and have erupted products of similar mineralogy and chemistry. No long-term chemical trends have characterised this period, but there is evidence of periodic short-lived departures to the eruption of different magma compositions (e.g. the basaltic andesite Angry Bird pumice (and the lava flow directly beneath it; an unusual style of effusive activity on Montserrat) in the earliest stages of Centre Hills, the dacitic Attic pumice at the end of Centre Hills, and the South Soufrière Hills episode). These departures mark transitions in the magma system, occurring near the start and at the end of Centre Hills activity, and marking a shift in stable phase assemblage at Soufrière Hills each side of the South Soufrière Hills episode.

The clinopyroxene-hypersthene andesites at Centre Hills are very similar in bulk composition to those from both Soufrière Hills Episodes 2 and 3, and petrographically similar to those from Episode 2. Incompatible trace element patterns for both volcanoes have comparable trough-shaped patterns related to MREE removal by amphibole crystallisation (Figure 14), supporting an interpretation of comparable magma-genetic processes between the two systems (cf. Cassidy et al., 2012). The eruption of hypersthene-hornblende andesites in Soufrière Hills Episode 3 was not associated with a change in bulk compositions. The only comparable transition at Centre Hills occurs in the youngest eruption at the volcano (the Attic pumice), and is associated with a change in bulk chemistry to more silicic compositions. The presence of amphibole in the Attic pumice may reflect cooling of the magma reservoir, promoting amphibole stability (hornblende becomes unstable at >880 °C at upper crustal pressures in Montserrat's andesite magmas (Barclay et al., 1998; Devine et al., 2003). Our limited number of estimated magma storage temperatures for Centre Hills suggests higher temperatures for magmas feeding explosive eruptions at Centre Hills (900-1000° C) than those estimated for the recent Soufrière Hills eruption (based on Fe-Ti oxide temperature estimates of ~870° C; Christopher et al., 2014), and it is possible that there is a temperature related control on both the stable phenocryst assemblage and the dominant eruptive style on Montserrat, although this interpretation requires further investigation.

The youngest (<24 ka; older units from Soufrière Hills have not been studied in great detail) products of Soufrière Hills show a notable difference in the abundance and composition of enclaves when compared with the Centre Hills explosive eruption deposits. At Soufrière Hills, mafic enclaves occur within lithic and pumice clasts and make up 1–12 vol.% of recent (1995-2010) eruptive products (Plail et al., 2014). These enclaves are interpreted as evidence of late-stage intrusion of mafic magma into the upper crustal storage region, resulting in mingling and localised heating (Barclay et al., 1998; Humphreys et al., 2009). Within the Centre Hills units we found no evidence of this process and no mafic enclaves; all enclaves in the pumice clasts are andesitic, with a similar mineralogy to the rest of Centre Hills deposits, suggesting that a different process was driving the large explosive eruptions at Centre Hills.

Although large explosive eruptions occurred throughout the Centre Hills period, effusive, lava-dome forming eruptions occurred alongside these, and lithic deposits from these eruptions comprise the bulk of the exposed stratigraphy around Centre Hills. A number of factors influence the explosivity of eruptions, including melt composition, gas content, magma viscosity, temperature, and vent and conduit geometries (Wilson et al., 1980; Scandone et al., 2007; Koleszar et al., 2012; Nguyen et al., 2014). Identifying a particular cause of the difference in behaviour between the two volcanoes is therefore difficult, although the dominant magma composition has been constant on Montserrat throughout the past million years, suggesting that magma composition is not the driver of changes in eruption style. Explosive eruptions are observed throughout the history of Centre Hills, even through periods of possible migration of the vent site, and there is no evidence to suggest that the dominant style of eruption is related to the maturity of the magma system or the size of the overlying edifice (e.g., Pinel and Jaupart, 2000; Taisne and Jaupart, 2008). The difference in enclave content, noted above, may mark a significant difference in the typical eruption triggering process, and our observations of hornblende stability and limited thermometry suggest that the current Soufrière Hills system may be cooler than the Centre Hills system. It is possible that temperature-related differences in viscosity and ascent behaviour enabled explosive eruption styles at Centre Hills, but this inference remains speculative.

## 5. Conclusions

This study substantially extends the stratigraphic record of volcanic activity on Montserrat, identifying several distinct episodes of volcanism since 1 Ma, characterised by shifts in vent site or dominant eruption style. We identify 11 thick (>1 m) pumiceous units (and a similar number of less well exposed units) derived from sustained explosive eruptions of the Centre Hills volcano, some of which have likely tephra volumes of >1 $km^3$ (e.g., Woodlands Bay pumice). The presence of multiple pumiceous deposits, interbedded with andesite lava breccias derived from effusive eruptions, implies that there were repeated sustained explosive eruptions throughout the lifetime of Centre Hills, alongside effusive, lava-dome forming eruptions. The volcanic rocks erupted throughout this period are andesites with very similar bulk chemical and mineralogical compositions. The final explosive eruption of Centre Hills, the Attic pumice eruption, departs from this pattern and has a dacitic composition.

Following the Attic pumice eruption, activity moved southwards to the Soufrière Hills volcano. The earlier stages of Soufrière Hills activity erupted andesites of very similar composition to the Centre Hills rocks, with evidence of periods of sustained explosive activity alongside more common effusive eruptions. Following the basaltic South Soufrière Hills episode at ~130 ka, activity at Soufrière Hills switched to predominantly effusive activity, without large explosive eruptions. The magma erupted in this final episode has identical bulk compositions to preceding andesitic activity, but has a hypersthenes-hornblende phenocryst assemblage, in contrast to the clinopyroxene-hypersthene assemblage that characterises earlier episodes of andesitic volcanism on Montserrat.

The notably greater propensity towards explosive volcanism at Centre Hills contrasts with a marked absence of similar activity at Soufrière Hills, especially since ~130 ka. An additional difference is the common occurrence of mafic enclaves in the Soufrière Hills rocks, which are absent in the pumiceous deposits from Centre Hills. The bulk composition of the erupted andesite has remained very similar on Montserrat since 1 Ma. This compositional stability suggests that local changes in magma storage conditions (potentially causing small differences in magma temperature or viscosity) and pre-eruptive dynamics, rather than shifts in magma composition, are the major control on eruption style during prolonged ($10^5$ year timescales) episodes of volcanism on Montserrat.

**6. Acknowledgments**

We thank the Montserrat Volcano Observatory for support during fieldwork, and Paul Cole, Eliza Calder, Ben Edwards, Rod Stewart and Adam Stinton for advice on field sites. Ar-Ar dates were funded by the NERC Isotope Geosciences Facility allocation IP-1401-1113. We thank Jim Imlach for assistance in sample preparation and dating, and Agnes Michalik, Ben Buse, Stuart Kearns and Ian Croudace for assistance with geochemical analyses. We acknowledge funding from NERC grants NE/K000403/1 and NE/I02044X/1 (SW) and Humboldt fellowship (MC).

**7. References**

Bacon, C.R., Lanphere, M.A., 2006. Eruptive history and geochronology of Mount Mazama and the Crater Lake region, Oregon. Geological Society of America Bulletin 118, 1331-1359.

Baker, P.E., 1985. Volcanic hazards on St Kitts and Montserrat, West Indies. Journal of the Geological Society of London 142, 279-295.

Barclay, J., Rutherford, M.J., Caroll, M.R., 1998. Experimental phase equilibria constraints on pre-eruptive storage conditions of the Soufrière Hills magma. Geophysical Research Letters 25, 3437-3440.

Mark, D.M., Barfod, D.N., Stuart, F.M., Imlach, J., 2009. The ARGUS multi-collector noble gas mass spectrometer: Performance for $^{40}Ar/^{39}Ar$ geochronology. Geochemistry Geophysics Geosystems 10 (1-13).

Branney, M.J., Kokelaar, B.P., 2002. Pyroclastic density currents and the sedimentation of ignimbrites. Geological Society, London, Memoirs, 27.

Brown, K., Davidson, C., 2008. $^{40}Ar/^{39}Ar$ geochronology of the Silver Hills andesite, Montserrat, West Indies. B.A. Senior Integrative Exercise, Carelton College, Northfield, Minnesota.

Brown, R.J., Civetta, L., Arienzo, I., D'Antonio, M., Moretti, R., Orsi, G., Tomlinson, E. L., Albert, P.G., Menzies, M.A., 2014. Geochemical and isotopic insights into the assembly, evolution and disruption of a magmatic plumbing system before and after a cataclysmic caldera-collapse eruption at Ischia volcano (Italy). Contributions to Mineralogy and Petrology 168, 1-23.

Cassidy, M., Taylor, R.N., Palmer, M.R., Cooper, R.J., Stenlake, C., Trofimovs, J., 2012. Tracking the magmatic evolution of island arc volcanism: Insights from a high-precision Pb isotope record of Montserrat, Lesser Antilles. Geology, Geochemistry, Geophysics 13, 1525-2027.

Cassidy, M., Watt, S.F.L., Palmer, M.R., Trofimovs, J., Symons, W., Maclachlan, S.E., Stinton, A.J., 2014a. Construction of volcanic records from marine sediment cores: A review and case study (Montserrat, West Indies). Earth-Science Reviews 138, 137-155.

Cassidy, M., Trofimovs, J., Watt, S.F.L., Palmer, M.R., Taylor, R.N., Gernon, T.M., Talling, P.J., Le Friant, A., 2014b. Multi-stage collapse events in the South Soufrière Hills, Montserrat, as recorded in marine sediment cores. Geological Society, Memoirs, 39, 383-397.

Cassidy, M., Watt, S.F.L., Talling, P.J., Palmer, M.R., Edmonds, M., Jutzeler, M., Wall-Palmer, D., Manga, M., Coussens, M., Gernon, T., Taylor, R.N., Michalik, A., Inglis, E., Breitkreuz, C., Le Friant, A., Ishizuka, O., Boudon, G., McCanta, M.C., Adachi, T., Hornbach, M.J., Colas, S.L., Endo, D., Fujinawa, A., Kataoka, K.S., Maeno, F., Tamura, Y., Wang, F., 2015, Rapid onset of mafic magmatism facilitated by volcanic edifice collapse. Geophysical Research Letters 42, 4778-4785.

Christopher, T.E., Humphreys, M.C., Barclay, J., Genareau, K., De Angelis, S.M., Plail, M., Donovan, A., 2014. Petrological and geochemical variation during the Soufrière Hills eruption, 1995 to 2010. Geological Society, Memoirs, 39, 317-342.

Coussens, M.F., Wall-Palmer, D., Talling, P.J., Watt, S.F.L., Cassidy, M., Jutzeler, M., Clare, M.A., Hunt, J.E., Manga, M., Gernon, T.M., Palmer, M.R., Hatter, S.J., Boudon, G., Endo, D., Fujinawa, A., Hatfield, R., Hornbach, M.J., Ishizuka, O., Kataoka, K., Le Friant, A., Maeno, F., McCanta, M., Stinton, A.J., 2016a. The relationship between eruptive activity, flank collapse and sea-level at volcanic

islands: a long-term (>1 Ma) record offshore Montserrat, Lesser Antilles. Geochemistry, Geophysics, Geosystems 17, 2591-2611.
Coussens, M.F., Wall-Palmer, D., Talling, P.J., Watt, S.F.L., Hatter, S.J., Cassidy, M., Clare, M., Jutzeler. M., Hatfield, R., McCanta, M., Kataoka, K.S., Endo, D., Palmer, M.R., Stinton.A., Fujinawa, A., Boudon, G., Le Friant, A., Ishizuka, O., Gernon, T., Adachi. T., Aliahdali, M., Breitkreuz, C., Frass, A., Hornbach M.J., Lebas, E., Lafuerza, S., Maeno, F., Manga, M., Martinez-Colon, M., MnManus, J., Morgan, S., Saito, T., Slagle, A., Subramanyam, K.S.V., Tamura, Y., Trofimovs, J., Villemant, B., Wang, F., and the expedition 340 scientists., 2016b. Synthesis: stratigraphy and age control for IODP Sites U1394, U1395, and U1396 offshore Montserrat in the Lesser Antilles. Proceedings of the Integrated Ocean Drilling Program, Volume 340, Le Friant, A., Ishizuka, O., Stroncik, N.A., and the Expedition 340 Scientists. doi:10.2204/iodp.proc.340.204.2016
Devine, J.D., Rutherford, M.R., Norton, G.E., Young, S.R., 2003. Magma storage region processes inferred from geochemistry of Fe-Ti oxides in andesitic magma, Soufrière Hills Volcano, Montserrat, W.I. Journal of Petrology 44, 1375-1400.
Druitt, T.H., Mellors, R.A., Pyle, D.M., Sparks, R.S.J., 1989. Explosive volcanism on Santorini, Greece. Geological Magazine 126, 95-126.
Druitt, T.H., Kokelaar, B.P., 2002. The eruption of Soufrière Hills Volcano, Montserrat, from 1995 to 1999. Geological Society, London, Memoirs, 21.
Edmonds, M., Pyle, D., Oppenheimer, C., 2001. A model for degassing at the Soufrière Hills Volcano, Montserrat, West Indies, based on geochemical evidence. Earth and Planetary Science Letters 186, 159-173.
Germa. A., Quidelleur, X., Lahitte, P., Labanieh, S., Chauvel, C., 2011. The K-Ar Cassignol-Gillot technique applied to western Martinique lavas: A record of Lesser Antilles arc activity from 2 Ma to Mount Pelée volcanism. Quaternary Geology 6, 341-355.
Harford, C.L., Pringle, M.S., Sparks, R.S.J., Young, S.R., 2002. The volcanic evolution of Montserrat using $^{40}Ar/^{39}Ar$ geochronology. Geological Society, Memoirs, 21, 93-113.
Humphreys, M.C.S., Blundy, J.D., Sparks, R.S.J., 2006. Magma evolution and open-system processes at Shiveluch volcano: insights from phenocryst zoning. Journal of Petrology 47, 2303-2334.
Humphreys, M.C.S., Christopher, T., Hards, V., 2009. Microlite transfer by disaggregation of mafic inclusions following magma mixing at Soufrière Hills volcano, Montserrat. Contributions to Mineralogy and Petrology 157, 609-624.
Koleszar. A.M., Kent, A.J.R., Wallace, P.J., Scott, W.E., 2012. Controls on long-term low explosivity at andesitic arc volcanoes: insights from Mount Hood, Oregon. Journal of Volcanology and Geothermal Research 219-220, 1-14.
Legros, F., 2000. Minimum volume of a tephra fallout deposit estimated from a single isopach. Journal of Volcanology and Geothermal Research 96, 25-32.
Lowe. D.J., 2011. Tephrochronology and its application: A review. Quaternary Geology 6, 107-153.
Nguyen. C.T., Gonnermann, H.M., Houghton, B.F., 2014. Explosive to effusive transition during the largest volcanic eruption of the 20th century (Novarupta 1912, Alaska). Geology 42, 703-706.
Pinel, V., Jaupart, C., 2000. The effect of edifice load on magma ascent beneath a volcano. Philosophical Transactions of the Royal Society, A 358, 1515-1532.

Plail. M., Barclay, J., Humphreys, M.C.S., Edmonds, M., Herd, R.A., Christopher, T.E., 2014. Characterization of mafic enclaves in the erupted products of Soufrière Hills Volcano, Montserrat, 2009 to 2010. Geological Society, Memoirs 39, 343-360.

Putirka, K., Johnson, M., Kinzler, R., Longhi, J., Walker, D., 1996. Thermobarometry of mafic igneous rocks based on clinopyroxene-liquid equilibria, 0–30 kbar. Contributions to Mineralogy and Petrology 123, 92-108.

Putirka, K.D., Mikaelian, H., Ryerson, F., Shaw, H., 2003. New clinopyroxene-liquid thermobarometres for maric, evolved, and volatile-bearing lava compositions, with applications to lavas from Tibet and the Snake River Plain, Idaho. American Mineralogist 88, 1542-1554.

Putirka, K.D., 2005. Mantle potential temperatures at Hawaii, Iceland, and the mid-ocean ridge system, as inferred from olivine phenocrysts: evidence for thermally driven mantle plumes. Geochemistry, Geophysics, Geosystems 6, 5.

Putirka, K.D., 2008. Thermometres and barometres for volcanic systems. In: Putirka, K.D., Tepley, F.J.I. (Eds.), Minerals, Inclusions, and Volcanic Processes. Mineralogical Society of America, pp. 61-120.

Pyle, D.M., 1999. Widely dispersed Quaternary tephra in Africa. Global and Planetary Change 21, 95-112.

Pyle, D.M., 2000. Sizes of volcanic eruptions. In: Sigurdsson, H., Houghton, B., Rymer, H., Stix, J., McNutt, S. (Eds.), Encyclopedia of Volcanoes. Academic Press, pp. 263-269.

Rea, W.J., 1975. The volcanic geology and petrology of Montserrat, West Indies. Journal of the Geological Society of London 130, 341-366.

Renne, P.R., Balco, G., Ludwig, K.R., Mundil, R., Min, K., 2011. Response to the comment by W.H. Schwarz et al. on “Joint determination of K-40 decay constants and Ar-40*/K-40 for the Fish Canyon sanidine standard, and improved accuracy for Ar-40/Ar-39 geochronology” by PR Renne, et al. 2010. Geochimica et Cosmochimica Acta 75,17, 5097e5100.

Ridolfi, F., Renzulli, A., Puerini, M. (2010). Stability and chemical equilibrium of amphibole in calc-alkaline magmas: an overview, new thermobarometric formulations and application to subduction-related volcanoes. Contributions to Mineralogy and Petrology 160, 45-66.

Roobol, M.J., Smith, A.L., 1998. Pyroclastic stratigraphy of the Soufrière Hills volcano, Montserrat - implications for the present eruption. Geophysical Research Letters 25, 3393-3396.

Scandone, R., Cashman, K.V., Malone, S.D., 2007. Magma supply, magma ascent and the style of volcanic eruptions. Earth and Planetary Science Letters 253, 513-529.

Singer, B.S., Jicha, B.R., Harper, M.A., Naranjo, J.A., Lara, L.E., Moreno-Roa, H., 2008. Eruptive history, geochronology, and magmatic evolution of the Puyehue-Cordón Caulle volcanic complex, Chile. Geological Society of America Bulletin 120, 599-618.

Smith, A.L., 2007. Prehistoric stratigraphy of the Soufrière Hills-South Soufrière Hills volcanic complex, Montserrat, West Indies. The Journal of Geology 115, 115-127.

Sparks, R.S.J.,Folkes, C.B., Humphreys, M.C.S., Barfod, D.N., Clavero, J., Sunagua, M.C., McNutt, S.R., Pritchard, M.E. 2008. Uturuncu volcano, Bolivia: Volcanic unrest due to mid-crustal magma intrusion. American Journal of Science 308, 6, 727-769.

Taisne, B., Jaupart, C., 2008. Magma degassing and intermittent lava dome growth. Geophysical Research Letters 35, L20310.

Trofimovs, J., Talling, P.J., Fisher, J.K., Hart, M.B., Sparks, R.S.J., Watt, S.F.L., Cassidy, M., Smart, C.W., Le Friant, A., Moreton S.G., Lang, M.J., 2013. Timing, origin and emplacement dynamics of mass flows offshore of SE Montserrat in the last 110 ka: Implications for landslide and tsunami hazards, eruption history, and volcanic island evolution. Geochemistry, Geophysics, Geosystems 14, 385-406.

Wadge, G., Isaacs, M.C., 1988. Mapping the volcanic hazards from Soufrière Hills volcano, Montserrat, West Indies using an image processor. Journal of the Geological Society 145, 541-551.

Wadge. G., Voight, B., Sparks, R.S.J., Cole, P.D., Loughlin, S.C., Robertson, R.E.A., 2014. An overview of the eruption of Soufrière Hills Volcano, Montserrat from 2000 to 2010. Geological Society, Memoirs, 39, 1-39.

Watt, S.F.L., Talling, P.J., Vardy, M.E., Masson, D.G., Henstock, T.J., Hühnerbach, V., Minshull, T.A., Urlaub, M., Lebas, E., Le Friant, A., Berndt, C., Crutchley, G.J., Karstens, J., 2012. Widespread and progressive seafloor-sediment failure following volcanic debris avalanche emplacement: Landslide dynamics and timing offshore Montserrat, Lesser Antilles. Marine Geology 323-325, 69-94.

White. J.D.L., Houghton, B.F., 2006. Primary volcaniclastic rocks. Geology 34, 677-680.

Wilson, L., Sparks, R.S.J., Walker, G.P.L., 1980. Explosive volcanic eruptions—IV. The control of magma properties and conduit geometry on eruption column behaviour. Geophysical Journal of the Royal Astronomical Society 63, 117-148.

Zellmer, G.F., Hawkesworth, C.J., Sparks, R.S.J., Thomas, L.E., Harford, C.L., Brewer, T.S., Loughlin, S.C., 2003. Geochemical evolution of the Soufrière Hills volcano, Montserrat, Lesser Antilles volcanic arc. Journal of Petrology 44, 1349-1374.

**Figure Captions**

**Figure 1:** Map of Montserrat showing the volcanic centres and selected geographic locations. All field sites are shown as circles, with the numbers indicating the location of specific samples, named in the key and shown in stratigraphic context in Figures 2 and 3.

**Figure 2:** Summary stratigraphic logs for sites west of Centre Hills (the most northerly site is at the left of the figure). Clast types and their relative concentration and sorting are shown schematically within each unit. Pumiceous deposits are identified as coloured bands. In many cases deposits form discontinuous horizons, and their correlation between sites has been based on physical characteristics (appearance, grain size, internal structure and stratigraphic order), confirmed in some cases by chemical analysis. Pumiceous units are separated by undifferentiated sequences of andesite lava breccias. Stratigraphic positions of samples (and the type of analysis, where relevant) are indicated. Full location details for all samples are provided in Supplementary Table 1.

**Figure 3:** Summary stratigraphic logs for sites east of Centre Hills (the most northerly site is at the left of the figure). Clast types and their relative concentration and sorting are shown schematically within each unit. Pumiceous deposits are identified as coloured bands. In many cases deposits form discontinuous horizons, and their correlation between sites has been based on physical characteristics (appearance, grain size, internal structure and stratigraphic order), confirmed in some cases by chemical analysis. Pumiceous units are separated by undifferentiated sequences of andesite lava breccias. Stratigraphic positions of samples (and the type of analysis, where relevant) are indicated. Full location details for all samples are provided as Supplementary Data.

**Figure 4:** Photographs of selected exposure of the pumice-rich units described here. Photo locations (latitude and longitude) and unit names are shown beneath each image. The tape measure, where shown, is extended to 1 m. The images show characteristic overall unit structures (e.g. Woodlands Bay image) or internal detail (e.g. pelletal lapilli in Attic Pumice), as well as the nature of the typical bounding stratigraphy for exposures throughout the study area (e.g. andesite lava breccias in Bransby Point and Angry Bird images).

**Figure 5:** Whole rock major element compositions plotted against silica for pumiceous units from central Montserrat. Most units have similar compositions and plot along a single fractional crystallisation trend. Nearly all units lie within the andesitic compositional field (bottom right) that typifies most volcanic rocks on Montserrat. The Attic pumice is more evolved, while the Angry Bird pumice is more mafic (although alteration may have affected the bulk chemistry of this unit).

**Figure 6:** Comparisons of a range of bulk-rock trace (upper panel) and major (lower panel) element concentrations against relative stratigraphic age (summarised on the right of each panel). All samples except the South Lime Kiln Bay pumice are of Centre-Hills age. Compositions are stable throughout the period represented, with the exception of the Angry Bird pumice and the slightly more evolved Attic pumice, which is the youngest recognised eruption from Centre Hills. There are subtle long term trends towards HREE depletion and HFSE enrichment (e.g. Th) in the youngest units.

**Figure 7:** Nd against Y for whole-rock trace element analyses of pumice for pyroclastic

units in central Montserrat. These elements allow several individual units to be discriminated on the basis of bulk chemistry, defining tight compositional clusters for several deposits (e.g. Garibaldi Hill and Old Road Bay pumices).

**Figure 8:** Ba/La and Th/La for volcanic systems on Montserrat (adapted from Cassidy et al., 2012). The basaltic South Soufrière Hills lies in a separate compositional field, and Soufrière Hills rocks have slightly higher Ba/La values than those from Centre Hills and Silver Hills, which lie in the same compositional field. Samples from this study all lie on the Centre and Silver Hills trend, but at slightly higher Th/La values.

**Figure 9:** Major element analyses of pyroxene phenocryst compositions from pumice clasts in selected Centre Hills deposits. Panel A shows the pyroxene phenocryst composition is very similar across all these units (rim and core compositions were highly similar and are not differentiated in this figure; full data are provided in Supplementary Table 2). Panel B shows Al and Fe compositions in the rims of clinopyroxene phenocrysts, indicating that subtle variations exist between some units and could potentially be used as a correlative tool.

**Figure 10:** Major element glass composition for pumice clasts from pyroclastic units in central Montserrat. For several units pumices clasts were analysed from multiple field sites (e.g. Attic and Garibaldi Hill pumices), and the similarity in glass composition between these sites supports their correlation. Although there is substantial overlap in glass composition for several units, reflecting their very similar bulk-rock chemistry, discrete fields can be defined for some deposits (e.g. Foxes and Bunkum Bay pumices). These units could potentially be used as marker beds for wider correlation between the subaerial and marine stratigraphy around Montserrat.

**Figure 11:** $^{40}Ar/^{39}Ar$ plateau ages plotted against cumulative percentage of Ar released for plagioclase phenocrysts separated from pumice clasts in six of the pyroclastic units studied here. Dashed lines show mean apparent age and solid lines show errors to 2σ at successive steps. The age obtained is shown at the top of each panel.

**Figure 12:** Approximate isopach sections constructed for the cumulative thickness of fall deposits within the more widely exposed pumiceous units identified from Centre Hills. Fall unit thicknesses used in constructing isopachs are shown in black text with location shown by green circles. Selected flow deposit thicknesses at the same sites are shown in red, with flow directions (based on the broad location of the assumed vent site) shown by red arrows. In the absence of other information, the vent site is assumed to be located at Katy Hill, although as discussed in the text, a more southerly vent site may have been the source of the older units described here, and is more consistent with the outcrop patterns of units such as the Bransby Point and Garibaldi Hill pumices.

**Figure 13:** A summary of the onshore stratigraphy of Montserrat over the past one million years, defining six episodes of volcanism separated by changes in vent site or eruptive behaviour. Schematic stratigraphic logs of representative subaerial sequences are shown for each episode (scales are approximate and are primarily representative of deposits found at the distal margins of the subaerial edifices). The top panel compares the episodes defined here with those defined in previous studies by Smith (2007) and Trofimovs et al. (2013).

**Figure 14:** Rare Earth element profiles showing the compositional range of analysed rocks from Centre Hills, Soufrière Hills and the South Soufrière Hills basaltic episode, adapted from Zellmer et al. (2003). Centre Hills rocks overlap entirely with those from Soufrière Hills, but show a broader compositional range.

**Table 1: Summary descriptions and interpretation of major pumice-rich deposits in central Montserrat**

| Unit | Extent of exposures | Type locality (latitude; longitude) | Unit samples | Sub-unit | Sub-unit lithofacies | Thickness, structure, grading | Lithological description | Interpretation of depositional process |
|---|---|---|---|---|---|---|---|---|
| | | | | | | | ***West of Centre Hills*** | |
| Attic Pumice | Laterally continuous along several road cuttings W of Centre Hills | N16.75413; E62.22226 | 8.1.1A, 3.3.1G, 3.2.1I+E, 3.2.1F, 3.1.8C | Upper | Cross-bedded tuff | 1.2 m, massive, with cross-bedded base. | Moderately sorted deposit dominated by subangular-subrounded pumice (90 vol.%) and ash-coated pelletal grains. Maximum pumice size 1 cm; lithics up to 3 cm. Lower part of the subunit contains fewer larger clasts (coarse-tail reverse sorting). | Primary deposit of low concentration PDC (presence of sedimentary structures; pelletal grains; homogeneous composition). |
| | | | | Middle | Tuff | 2 m, massive | Well-sorted, contains >90 vol.% of 2 mm pumice clasts and ash-coated clasts. | Primary deposit of wet (pelletal grains) tephra fall or possible low-moderate concentration PDC (well sorted, but without sedimentary structures). |
| | | | | Lower | Massive lapilli-tuff | 3 m, dm-bedded | Moderately to poorly sorted. Variable amounts of pumice clasts, lithics, pelletal grains, and ash. Clasts chiefly 2-5 mm in size. Contains single-clast-thick pumice horizons. Fewer pelletal grains at the base of the sub-unit. | Primary deposit of moderate concentration PDC (some bedding structures developed). |
| Woodlands Bay Pumice | Laterally continuous, can be traced along coastal cliffs on the west coast with individual exposures over ~500 m | N6.76298; E62.22343 | 5.1.1C, 5.1.1A, 5.1.1B, 10.1.1A, 3.1.2A+B , | Upper | Banded lapilli-tuff | 5 m, dm-bedded | Moderately sorted, angular lapilli. Comprises >95 vol.% pumice clasts (4.5 cm mean size, max clast size 18 cm), and <5 vol.% grey lithics (max 5 cm). Very little (<1 vol.%) finer-grained matrix. | Primary tephra fall (moderately well sorted, consistent thickness, angular clasts, pumice dominated). |
| | | | | Middle | Interbedded lapilli-tuff | 7 m, dm-m bedded | A sequence of decimetre pumice lapilli beds defined by ash-rich and ash-poor alternating beds. Ash rich beds: poor to moderately sorted, subangular, <40 vol.% ash matrix, 10-20 vol.% lithics, and up to 60 vol.% pumice lapilli, mean size 1 cm. Contains pumice lapilli lenses and single-clast-thick pumice horizons. Pumice rich: Moderately sorted, angular. Comprises 70-90 vol.% pumice clasts, 30 vol.% lithics, and 10 vol.% ash. Pumice mean size 2-4 cm, max 11 cm. | Primary tephra fall deposits (lapilli beds) interleaved with moderately concentrated PDC deposits (poor-moderate sorting; relatively high ash content). Some fall deposits may be reworked at the top by subsequent PDCs. |
| | | | | Lower | Lapilli-tuff | 4.5 m, dm-m bedded | Variably sorted, angular-subangular lapilli deposit, with wide variation in pumice lapilli content (20-90 vol.%), ash content (10-90 vol.%) and lithic content (10-50 vol.% ) between individual beds. Mean clast size 1-2cm. Occasional well sorted pumice lapilli lenses. | Deposit from high concentration PDCs, potentially with partial reworking. |
| Bunkum Bay Pumice | Crops out in isolated lenses (<50 m laterally), often as channelised sequences | N16.77193; E62.22037 | 6.1.4B, 6.1.2A, 3.4.2H | Upper | Lapilli-tuff | 7 m, massive, discordant basal contact. | Poorly-sorted, polymict deposit of pumice and lithic clasts. Detailed composition uncertain due to inaccessible outcrop. | Possibly reworked (e.g. laharic) deposit derived from underlying deposit. |
| | | | | Lower | Interbedded lapilli-tuff and tuff channels | 0-7m, channel deposits. | Alternating units of tuff and lapilli-tuff. Tuff units: moderate-well sorted, laminated with accretionary lapilli-rich (3mm) and pumice-rich horizons (up to 2 cm in size) in a matrix of orange medium-grained ash with 20 vol.% plagioclase and pyroxene crystals. Lapilli-tuff horizons: Poorly-sorted, angular. Comprises 65-90 vol.% pumice clasts (5 cm maximum size), 5-15 vol.% grey and altered lithics, and <5-20 vol.% coarse grey ash rich in plagioclase and pyroxene crystals. | Primary deposits of alternating high and low concentration phases of PDCs (alternation between well-sorted, laminated deposits to poorly- sorted deposits). Accretionary lapilli suggest wet environment. |

| | | | | | | | | |
|---|---|---|---|---|---|---|---|---|
| Foxes Pumice | Crops out in one isolated cliff section, traceable for ~50 m | N16.72365; E62.24035 | 4.2.5I, 4.2.2E | Upper | lapilli-tuff | 3 m, massive to dm-bedded. | Well-sorted, angular pumice lapilli (>90 vol.%; 2-5 mm in size) with <10 vol.% ash and <1 vol.% lithics. | Primary tephra fall (well sorted, dominated by angular pumice). |
| | | | | Lower | Tuff | 20 cm, laminated. | Well-sorted pink medium-grained ash. | Primary tephra fall or possibly low concentration density current. |
| Old Road Bay Tuff | Present from Old Road Bay to Lime Kiln Bay, thinning N. | N16.73722; E62.23302 | 2.1.2B | Upper | Bedded lapilli-Tuff | 1 m, cm-bedded. | Well sorted, subangular pumice lapilli within ash matrix, alternating between yellow ash beds and thin pumice horizons (1 cm beds; pumice maximum size 1 cm). | Primary tephra fall from pulsed eruption or low concentration PDC. |
| | | | | Lower | Tuff | 50 cm, dm-bedded | Well sorted, laminated tuff, laterally continuous. Top and base are grey, middle is yellow | Primary tephra fall (well sorted, laterally continuous) |
| Bransby Point Pumice | Laterally continuous for ~3 km around Bransby Point towards Plymouth | N16.72365; E62.24035 | BP | Upper | Massive lapilli-tuff | 1 m, massive | Well-sorted, angular pumice lapilli, with laterally consistent thickness. Comprises >90 vol.% of pink pumices (max 4.5 cm), 5 vol.% grey lithics (max 2.5 cm), and 5 vol.% pink ash. Some discontinuous 1 cm thick ash horizons within deposit. Capped by a thin (~5 cm) ash layer. | Primary tephra fall (well sorted angular clasts, pumice rich, laterally continuous). |
| | | | | Lower | Massive lapilli-tuff | 1 m, dm-bedded | Well-sorted, angular white pumice lapilli (>95 vol.%; max size 5 cm), 5 vol.% grey lithics, <1 vol.% white fine-medium ash. Capped by a thin (<10 cm) pink ash. | Primary tephra fall (well sorted angular clasts, pumice rich, laterally continuous). |
| Garibaldi Hill Pumice | Laterally continuous, thickening southwards. Tilted at Garibaldi Hill. | N16.72899 E62.23521 | 4.1.4H, 5.2.3E, 11.1.3B, 9.2.1C, 9.2.1D, 7.1.1A | Upper | Lapilli-tuff | 50 cm, massive. | Well-sorted, angular yellow pumice lapilli (95 vol.%; max size 4 cm), 5 vol.% lithics, and <1 vol.% yellow medium-grained ash. | Primary tephra fall (well sorted angular clasts, pumice rich, laterally continuous). |
| | | | | Lower | Normally graded lapilli-tuff | 5 m, normally graded | Sequence of poorly-sorted beds containing subangular-rounded lapilli in both lithic- and pumice-rich lenses, with individual beds comprising 50-80 vol.% pumice (max size 12 cm), 5-20 vol.% lithics, and <5-45 vol.% ash. | Primary high concentration PDC deposit (poor-sorting; lack of sedimentary structures). |
| Old Road Bay Pumice | Crops out on both the east and west coasts of Montserrat. | N16.72899; E62.23521 | 13.1.1A. 11.1.1A, 4.2.3G, 9.2.1F, 9.2.1G, 9.2.1H | Upper | Lapilli-tuff | 3.5 m, massive and normally graded | Moderately-poorly sorted bed with rounded lapilli. Comprises 50 vol.% yellow pumices clasts and lithics (difficult to distinguish due to weathering), and 50 vol.% coarse ash. | Primary deposit of high concentration PDC (poorly sorted, heterogeneous, rounded clasts). |
| | | | | Middle | Lapilli-tuff | <1 m, finely bedded | Alternating well-sorted ash and lapilli beds, with lamination in the ash layers. Coarser lapilli beds contain pumice and accretionary lapilli, with higher concentrations of pumice lapilli at the top of the unit. | Primary tephra fall from pulsed eruption, or series of low-medium concentration density currents (well-sorted deposits). |
| | | | | Lower | Lapilli-tuff | 1.5 m, massive with normally graded top | Moderately sorted, with rounded lapilli dominated by yellow pumice (>90 vol.%; max size 7cm) and <10 vol.% white ash matrix. | Primary pumice-rich low concentration PDC (homogenous, rounded clasts). |
| South Lime Kiln Bay Pumice | Crops out within an isolated faulted block | N16.74799; E62.23473 | 11.1.4C | Upper | Lapilli-tuff | >2 m, reversely graded | Poorly-sorted, subangular-subrounded lapilli beds with variable proportions of pumice and lithic clasts, comprising 15-85 vol.% pumice (2cm mean size, max size 5 cm), 5-75 vol.% grey, black and purple lithics, and 10 vol.% buff ash. Better sorting in pumice-rich base; proportion of lithic clasts, and lithic clast size increases towards the top. | Primary deposit of high concentration PDC (heterogeneous, poorly sorted), possibly reworked at top. |

| | | | | | | | | |
|---|---|---|---|---|---|---|---|---|
| | | | | Middle | Lapilli-tuff | 4 m, massive | Sequence of thin beds with moderate-poor sorting of subangular-subrounded lapilli and slightly variable proportions of pumice and lithic clasts (75->95 vol.% pumice lapilli (2 cm mean size, max size 15 cm), 5-10 vol.% assorted lithics and <1-20 vol.% ash). | Primary sequence of high concentration PDC deposits (poorly sorted units) and fall deposits (well sorted beds with angular clasts). |
| | | | | Lower | Lapilli-tuff | >1 m, massive | Poor-moderately sorted ash-rich beds with subangular pumice lapilli and lithic grains in variable proportions, comprising 5-30 vol.% pumice lapilli (2 cm mean size), 10-40 vol.% assorted lithics (3 cm mean size, max size 15 cm), and 60-90 vol.% coarse ash. The ash is red and comprises 30 vol.% plagioclase and pyroxene crystals. Fine-grained (weathered?) fiamme-shaped clasts also occur. | Primary deposit of high concentration PDC (poor-moderate sorting, coarse lithics, high ash content). |
| | | | | | ***East of Centre Hills*** | | | |
| Statue Rock | Laterally traceable along the cliff at Statue rock | N16.78158; E62.17855 | 13.4.1E. 13.3.1D | N/A | Lapilli-tuff | 10 m, low-angle cross bedding | Poorly sorted ash-rich deposit with rounded pumice lapilli and lithic lenses. Bedding defined by thin, elongate pumice lapilli lenses (one clast thickness). Total unit comprises 30 vol.% pumice lapilli (mean size 3 cm), 30 vol.% grey and black lithics (mean size 7 cm, max size ~1 m) and 40 vol.% coarse ash (containing ~30 vol.% pyroxene and plagioclase crystals). | High concentration PDC deposits, potentially partially reworked. |
| Bramble Pumice | Crops out in isolated lenses (<50 m lateral extent) | N16.76603; E62.16407 | 14.1.2B, 15.1.3A, 16.1.4C | N/A | Lapilli-tuff | 12 m, massive and reversely graded | Series of poorly-sorted lithic dominated units with subordinate lenses of angular-rounded pumice lapilli, often only one-clast thick. Pumice clasts range in size from 1-5 cm, with variable proportions throughout the unit (5-30 vol.%, except in lenses), the remainder a mix of lithics (30-50 vol.% ) and grey or orange medium-coarse ash (up to 85 vol.% in parts). The ash is often crystal rich (up to 30 vol.% plagioclase and pyroxene crystals). The unit also contains 30-50 cm sized rip-up clasts of laminated ash. | Largely reworked deposit (rip-up clasts, poor sorting) derived from PDC deposits. |
| Angry Bird Pumice | Traceable along much of the east coast, less continuous to the south | N16.77051; E62.16901 | 14.1.2.A, 13.1.2B | N/A | lapilli-tuff | 4.5 m, massive and normally graded | Series of up to 4 units separated by andesite lava breccias. Moderately-well sorted beds of angular-subangular pumice lapilli. Pumice clasts have a flattened shape and have mostly altered to clays. Beds comprise 85 vol.% white pumice (1 cm mean size, max size 3 cm), 5 vol.% grey and red lithics, and 10 vol.% pink coarse ash. The ash is crystal rich, consisting of 50 vol.% plagioclase and pyroxene crystals. | Primary tephra fall deposits (well-sorted, homogenous, angular clasts). |

**Table 2: Whole-rock major element analyses of pumice from pyroclastic units in central Montserrat (XRF, wt.%, normalised to 100% anhydrous compositions).**

| Sample | Unit | $SiO_2$ | $TiO_2$ | $Al_2O_3$ | $Fe_2O_3$ | MnO | MgO | CaO | $K_2O$ | $Na_2O$ | $P_2O_5$ | Mg# |
|---|---|---|---|---|---|---|---|---|---|---|---|---|
| **3.1.8C** | **Attic** | 65.39 | 0.42 | 16.72 | 5.13 | 0.14 | 1.99 | 5.77 | 1.12 | 3.22 | 0.11 | 60.61 |
| **8.1.1A** | **Attic** | 65.36 | 0.41 | 16.37 | 5.32 | 0.16 | 2.13 | 5.49 | 1.10 | 3.54 | 0.12 | 61.30 |
| **3.1.2 A +B** | **Woodlands Bay** | 62.27 | 0.54 | 17.77 | 6.23 | 0.15 | 2.38 | 6.44 | 0.91 | 3.26 | 0.05 | 60.22 |
| **5.1.1B** | **Woodlands Bay** | 61.33 | 0.61 | 17.64 | 6.88 | 0.16 | 2.51 | 6.57 | 0.91 | 3.29 | 0.10 | 59.04 |
| **3.4.2H** | **Bunkum Bay** | 62.87 | 0.46 | 17.56 | 5.58 | 0.14 | 2.30 | 6.25 | 1.04 | 3.73 | 0.09 | 61.98 |
| **13.4.1E** | **Statue Rock** | 58.66 | 0.59 | 19.38 | 7.68 | 0.18 | 2.46 | 6.95 | 0.60 | 3.40 | 0.10 | 55.96 |
| **BP 1** | **Bransby Point** | 61.60 | 0.53 | 17.65 | 6.79 | 0.16 | 2.24 | 6.77 | 0.90 | 3.26 | 0.13 | 56.63 |
| **BP 2** | **Bransby Point** | 59.14 | 0.53 | 17.45 | 7.02 | 0.18 | 2.87 | 7.07 | 0.87 | 4.34 | 0.15 | 61.82 |
| **7.1.1A** | **Garibaldi Hill** | 60.90 | 0.55 | 18.81 | 6.65 | 0.15 | 2.48 | 6.34 | 0.83 | 3.22 | 0.06 | 59.64 |
| **5.2.3 E** | **Garibaldi Hill** | 60.98 | 0.56 | 17.51 | 6.98 | 0.18 | 2.52 | 6.96 | 0.80 | 3.35 | 0.16 | 58.88 |
| **15.1.3A** | **Bramble** | 62.27 | 0.54 | 17.74 | 6.22 | 0.15 | 2.36 | 6.46 | 0.91 | 3.29 | 0.05 | 60.09 |
| **4.2.3G** | **Old Road Bay pumice** | 61.04 | 0.56 | 17.76 | 6.60 | 0.17 | 2.52 | 6.78 | 0.86 | 3.55 | 0.17 | 60.15 |
| **9.2.1 G** | **Old Road Bay pumice** | 59.86 | 0.57 | 19.15 | 6.69 | 0.15 | 2.45 | 6.93 | 0.70 | 3.44 | 0.07 | 59.17 |
| **13.1.1 A** | **Old Road Bay pumice** | 60.91 | 0.54 | 17.64 | 6.71 | 0.17 | 2.59 | 6.96 | 0.85 | 3.50 | 0.14 | 60.42 |
| **13.1.2 B** | **Angry Bird** | 52.30 | 0.84 | 21.29 | 10.42 | 0.32 | 4.59 | 7.41 | 0.24 | 2.46 | 0.13 | 63.58 |
| **11.1.4C** | **South Lime Kiln Bay** | 61.98 | 0.51 | 17.43 | 6.43 | 0.18 | 2.53 | 6.58 | 0.78 | 3.42 | 0.15 | 60.94 |
| **9.1.2 A** | un-named | 62.13 | 0.51 | 17.87 | 6.00 | 0.17 | 2.25 | 6.48 | 0.92 | 3.60 | 0.08 | 59.80 |
| **2.1.2 A** | un-named | 59.22 | 0.56 | 19.02 | 7.40 | 0.19 | 2.62 | 6.75 | 0.72 | 3.40 | 0.11 | 58.40 |
| **7.3.2C** | un-named | 61.94 | 0.53 | 17.90 | 6.06 | 0.15 | 2.28 | 6.77 | 0.91 | 3.36 | 0.11 | 59.87 |
| **5.2.1 D** | un-named | 58.27 | 0.86 | 15.30 | 9.45 | 0.21 | 4.99 | 7.14 | 1.16 | 2.44 | 0.17 | 67.65 |
| **9.2.1 E** | un-named | 58.21 | 0.68 | 19.38 | 9.32 | 0.17 | 2.99 | 5.89 | 0.28 | 3.00 | 0.09 | 55.93 |
| **12.1.4 B** | un-named | 56.80 | 0.72 | 18.67 | 7.42 | 0.14 | 3.45 | 8.54 | 0.90 | 3.23 | 0.11 | 64.82 |
| **16.1.2 A** | un-named | 60.19 | 0.52 | 17.86 | 6.52 | 0.16 | 2.56 | 6.83 | 0.84 | 4.38 | 0.14 | 60.82 |

**Table 3: Whole rock trace element chemistry of pumice from pyroclastic units in central Montserrat (solution ICP-MS, ppm)**

| Sample | Unit | Y | Sr | Ta | Nb | La | Ce | Pr | Nd | Sm | Eu | Dy | Ho | Er | Tm | Yb | Lu | Hf | Th |
|---|---|---|---|---|---|---|---|---|---|---|---|---|---|---|---|---|---|---|---|
| **3.2.1F** | **Attic** | 15.28 | 253.8 | 0.349 | 3.166 | 11.55 | 22.86 | 3.026 | 11.71 | 2.395 | 0.817 | 2.304 | 0.504 | 1.511 | 0.243 | 1.692 | 0.281 | 2.09 | 2.869 |
| **8.1.1A** | **Attic** | 16.05 | 256.9 | 0.614 | 3.501 | 12.85 | 26.72 | 3.26 | 12.5 | 2.519 | 0.811 | 2.369 | 0.515 | 1.552 | 0.252 | 1.808 | 0.303 | 2.243 | 3.325 |
| **3.1.8C** | **Attic** | 17.05 | 277.8 | 0.412 | 3.289 | 12.66 | 26.48 | 3.236 | 12.59 | 2.625 | 0.83 | 2.518 | 0.545 | 1.628 | 0.261 | 1.843 | 0.311 | 3.097 | 3.921 |
| **10.1.1 A** | **Woodlands Bay** | 22.36 | 241.1 | 0.441 | 3.361 | 10.84 | 22.96 | 3.138 | 12.87 | 2.933 | 0.961 | 3.323 | 0.73 | 2.206 | 0.361 | 2.593 | 0.429 | 3.399 | 3.339 |
| **3.1.2 A +B** | **Woodlands Bay** | 21.83 | 251.5 | 0.3 | 2.985 | 10.77 | 22.73 | 3.05 | 12.83 | 2.924 | 0.932 | 3.215 | 0.695 | 2.103 | 0.338 | 2.381 | 0.385 | 3.305 | 2.878 |
| **5.1.1B** | **Woodlands Bay** | 21.07 | 250.8 | 0.38 | 3.04 | 10.87 | 24.32 | 3.105 | 12.75 | 2.904 | 0.935 | 3.197 | 0.692 | 2.086 | 0.334 | 2.338 | 0.38 | 3.03 | 2.75 |
| **5.1.1A** | **Woodlands Bay** | 21.66 | 239.4 | 0.291 | 3.087 | 10.53 | 23.12 | 3.09 | 12.87 | 2.989 | 0.935 | 3.307 | 0.727 | 2.148 | 0.347 | 2.435 | 0.401 | 2.867 | 2.46 |
| **3.4.2H** | **Bunkum Bay** | 15.99 | 249 | 0.713 | 2.72 | 11.04 | 21.19 | 3.078 | 12.23 | 2.587 | 0.809 | 2.501 | 0.525 | 1.529 | 0.243 | 1.717 | 0.274 | 1.855 | 2.606 |
| **6.1.2 A** | **Bunkum Bay** | 18 | 216.8 | 0.304 | 2.928 | 9.446 | 20.74 | 2.918 | 12.18 | 2.734 | 0.83 | 2.934 | 0.628 | 1.879 | 0.297 | 2.089 | 0.338 | 2.566 | 2.003 |
| **4.2.5I** | **Foxes Bay** | 28.05 | 260.7 | 0.357 | 3.352 | 12.34 | 27.04 | 3.71 | 15.64 | 3.643 | 1.101 | 4.144 | 0.919 | 2.729 | 0.436 | 3.052 | 0.491 | 3.31 | 2.941 |
| **13.4.1E** | **Statue Rock** | 27.29 | 235.3 | 0.297 | 2.808 | 9.906 | 21.56 | 3.21 | 13.81 | 3.306 | 1.063 | 3.954 | 0.861 | 2.599 | 0.404 | 2.736 | 0.45 | 2.885 | 2.187 |
| **2.1.2B** | **Old Road Bay tuff** | 17.38 | 284.3 | 0.357 | 2.64 | 10.2 | 22.04 | 2.753 | 11.09 | 2.458 | 0.849 | 2.611 | 0.57 | 1.692 | 0.276 | 1.889 | 0.305 | 1.927 | 2.214 |
| **9.2.1 C** | **Garibaldi Hill** | 25.91 | 235.5 | 0.528 | 3.17 | 11.61 | 24.36 | 3.542 | 14.77 | 3.467 | 0.997 | 3.823 | 0.836 | 2.515 | 0.404 | 2.828 | 0.46 | 3.009 | 2.693 |
| **7.1.1A** | **Garibaldi Hill** | 24.55 | 238.7 | 1.684 | 3.132 | 12.21 | 23.49 | 3.544 | 15.08 | 3.42 | 1.018 | 3.696 | 0.806 | 2.388 | 0.383 | 2.699 | 0.439 | 3.04 | 2.754 |
| **4.1.4H** | **Garibaldi Hill** | 24.98 | 271.4 | 0.337 | 3.08 | 10.47 | 24.18 | 3.272 | 13.9 | 3.353 | 1.059 | 3.88 | 0.843 | 2.534 | 0.401 | 2.832 | 0.452 | 2.838 | 2.098 |
| **5.2.3 E** | **Garibaldi Hill** | 25.01 | 278.8 | 1.312 | 3.095 | 11.34 | 25.48 | 3.373 | 14.23 | 3.362 | 1.089 | 3.754 | 0.824 | 2.478 | 0.393 | 2.701 | 0.438 | 3.235 | 2.465 |
| **11.1.3 B** | **Garibaldi Hill** | 26.5 | 261.8 | 0.29 | 2.713 | 12.61 | 24.58 | 3.483 | 14.71 | 3.308 | 1.006 | 3.927 | 0.856 | 2.542 | 0.402 | 2.77 | 0.439 | 2.655 | 2.357 |
| **15.1.3A** | **Bramble** | 22.31 | 246.8 | 0.335 | 2.725 | 10.1 | 22.67 | 3.113 | 13.19 | 3.064 | 0.955 | 3.404 | 0.727 | 2.187 | 0.352 | 2.417 | 0.389 | 2.651 | 2.033 |
| **16.1.4C** | **Bramble** | 19.41 | 256.1 | 0.943 | 2.605 | 9.011 | 20.2 | 2.855 | 12.23 | 2.875 | 0.936 | 3.016 | 0.64 | 1.906 | 0.306 | 2.104 | 0.337 | 2.387 | 1.744 |
| **14.1.2 B** | **Bramble** | 20.38 | 211.6 | 0.473 | 2.7 | 9.841 | 21.9 | 2.886 | 12 | 2.741 | 0.84 | 3.056 | 0.667 | 2.009 | 0.324 | 2.223 | 0.352 | 2.673 | 2.31 |
| **9.2.1 H** | **Old Road Bay** | 21.71 | 244.4 | 0.269 | 2.431 | 9.483 | 20.34 | 2.886 | 12.13 | 2.906 | 0.87 | 3.303 | 0.709 | 2.116 | 0.332 | 2.305 | 0.37 | 2.568 | 2.15 |
| **9.2.1F** | **Old Road Bay** | 20.25 | 257.2 | 0.268 | 2.805 | 9.332 | 21.27 | 2.808 | 12.13 | 2.9 | 0.968 | 3.172 | 0.678 | 2.02 | 0.327 | 2.279 | 0.36 | 2.866 | 2.09 |
| **9.2.1 G** | **Old Road Bay** | 20.97 | 301 | 0.27 | 2.865 | 8.883 | 19.99 | 2.639 | 11.38 | 2.821 | 0.969 | 3.219 | 0.711 | 2.126 | 0.347 | 2.431 | 0.393 | 3.077 | 2.213 |

| | | | | | | | | | | | | | | | | | | | |
|---|---|---|---|---|---|---|---|---|---|---|---|---|---|---|---|---|---|---|---|
| **11.1.1A** | **Old Road Bay** | 19.56 | 220.9 | 0.414 | 2.684 | 10.12 | 22.28 | 2.835 | 11.64 | 2.645 | 0.839 | 2.975 | 0.64 | 1.934 | 0.312 | 2.192 | 0.354 | 2.73 | 2.536 |
| **4.2.3G** | **Old Road Bay** | 20.35 | 233 | 1.315 | 2.721 | 8.985 | 20.67 | 2.789 | 11.95 | 2.841 | 0.912 | 3.306 | 0.706 | 2.139 | 0.343 | 2.393 | 0.387 | 2.04 | 1.569 |
| **13.1.2 B** | **Angry Bird** | 34.8 | 236.7 | 0.549 | 3.751 | 15.06 | 26.34 | 4.322 | 18.38 | 4.592 | 1.407 | 5.567 | 1.175 | 3.43 | 0.536 | 3.686 | 0.576 | 3.285 | 2.971 |
| **11.1.4C** | **South Lime Kiln Bay** | 33.89 | 262.8 | 0.284 | 2.944 | 10.64 | 24.43 | 3.606 | 16.42 | 4.157 | 1.189 | 4.828 | 1.036 | 3.104 | 0.482 | 3.296 | 0.517 | 2.885 | 2.202 |
| **9.1.2 A** | un-named | 31.07 | 236.9 | 0.351 | 3.001 | 11.1 | 23.33 | 3.822 | 17.43 | 4.261 | 1.223 | 4.613 | 1.023 | 3.181 | 0.525 | 3.794 | 0.639 | 2.871 | 2.577 |
| **7.3.2C** | un-named | 29.41 | 232.9 | 0.406 | 2.954 | 15.09 | 23.41 | 4.51 | 19.57 | 4.34 | 1.282 | 4.352 | 0.953 | 2.768 | 0.442 | 3.011 | 0.483 | 2.63 | 2.505 |
| **12.1.6C** | un-named | 18.39 | 226.7 | 0.441 | 2.823 | 8.002 | 17.36 | 2.299 | 9.956 | 2.408 | 0.88 | 2.832 | 0.614 | 1.851 | 0.296 | 2.098 | 0.337 | 2.804 | 2.058 |
| **16.1.5D** | un-named | 20.69 | 223.6 | 0.237 | 2.526 | 9.436 | 20.74 | 2.952 | 12.72 | 2.94 | 0.895 | 3.169 | 0.677 | 1.997 | 0.328 | 2.224 | 0.357 | 2.424 | 1.866 |
| **2.1.2 A** | un-named | 20.73 | 282.8 | 0.306 | 2.834 | 9.032 | 20.96 | 2.894 | 12.7 | 2.999 | 1.057 | 3.231 | 0.692 | 2.062 | 0.329 | 2.26 | 0.37 | 2.812 | 1.93 |
| **4.2.3F** | un-named | 21.97 | 273.1 | 1.25 | 2.493 | 9.313 | 21.21 | 2.907 | 12.66 | 3.143 | 1.004 | 3.502 | 0.741 | 2.224 | 0.346 | 2.335 | 0.364 | 2.484 | 1.899 |
| **16.1.2 A** | un-named | 16.3 | 196.6 | 0.22 | 2.315 | 7.361 | 16.85 | 2.247 | 9.385 | 2.245 | 0.738 | 2.522 | 0.545 | 1.669 | 0.262 | 1.848 | 0.305 | 2.093 | 1.534 |
| **9.2.1 E** | un-named | 16.27 | 224.3 | 0.354 | 2.858 | 7.178 | 19.18 | 2.408 | 10.34 | 2.492 | 1.131 | 2.69 | 0.56 | 1.647 | 0.262 | 1.861 | 0.299 | 2.274 | 1.818 |
| **12.1.1A** | un-named | 16.08 | 326.7 | 0.321 | 1.531 | 6.008 | 13.24 | 1.778 | 7.862 | 2.082 | 0.771 | 2.7 | 0.569 | 1.612 | 0.24 | 1.594 | 0.242 | 1.18 | 1.242 |

**Table 4: Estimated minimum deposit volumes (tephra volume) for selected fall deposits (cf. Pyle, 1999)**

| Unit | Isopach thickness (m) | Isopach area ($km^2$) | Deposit volume ($km^3$) |
|---|---|---|---|
| **Attic** | 0.3 | 20 | 0.02 |
| **Woodlands Bay** | 4 | 29 | 0.43 |
| **Old Road Bay tuff** | 0.6 | 19 | 0.04 |
| **Bransby Point** | 1 | 63 | 0.23 |
| **Garibaldi Hill** | 0.6 | 62 | 0.14 |
| **Old Road Bay pumice** | 0.3 | 30 | 0.03 |
| **Angry Bird** | 1 | 49 | 0.18 |

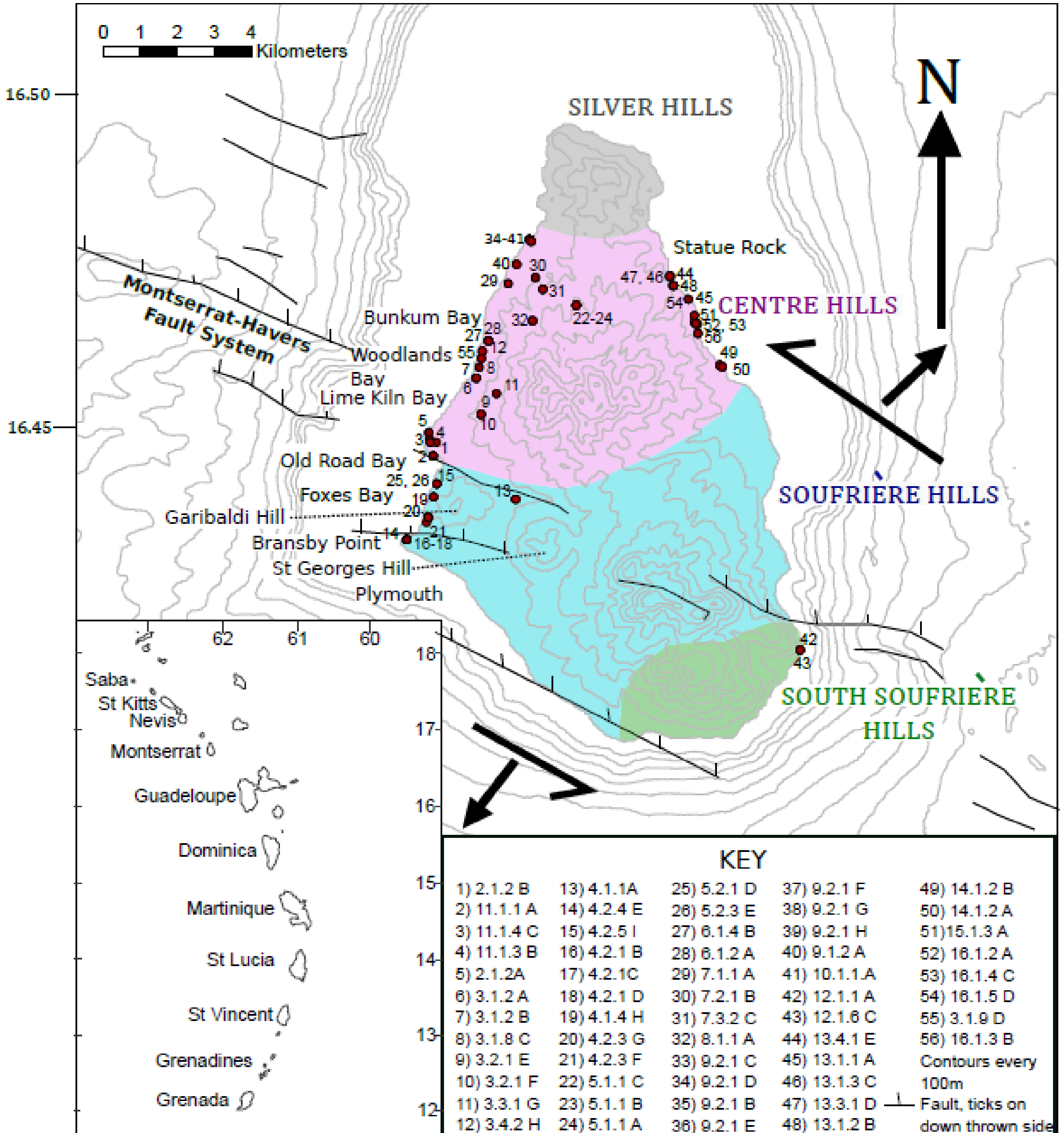
0 1 2 3 4
Kilometers
16.50
16.45
N
SILVER HILLS
CENTRE HILLS
SOUFRIÈRE HILLS
SOUTH SOUFRIÈRE HILLS
Statue Rock
Montserrat-Havers Fault System
Bunkum Bay
Woodlands Bay
Lime Kiln Bay
Old Road Bay
Foxes Bay
Garibaldi Hill
Bransby Point
St Georges Hill
Plymouth
62
61
60
18
17
16
15
14
13
12
Saba
St Kitts
Nevis
Montserrat
Guadeloupe
Dominica
Martinique
St Lucia
St Vincent
Grenadines
Grenada
KEY
1) 2.1.2 B
2) 11.1.1 A
3) 11.1.4 C
4) 11.1.3 B
5) 2.1.2A
6) 3.1.2 A
7) 3.1.2 B
8) 3.1.8 C
9) 3.2.1 E
10) 3.2.1 F
11) 3.3.1 G
12) 3.4.2 H
13) 4.1.1A
14) 4.2.4 E
15) 4.2.5 I
16) 4.2.1 B
17) 4.2.1C
18) 4.2.1 D
19) 4.1.4 H
20) 4.2.3 G
21) 4.2.3 F
22) 5.1.1 C
23) 5.1.1 B
24) 5.1.1 A
25) 5.2.1 D
26) 5.2.3 E
27) 6.1.4 B
28) 6.1.2 A
29) 7.1.1 A
30) 7.2.1 B
31) 7.3.2 C
32) 8.1.1 A
33) 9.2.1 C
34) 9.2.1 D
35) 9.2.1 B
36) 9.2.1 E
37) 9.2.1 F
38) 9.2.1 G
39) 9.2.1 H
40) 9.1.2 A
41) 10.1.1.A
42) 12.1.1 A
43) 12.1.6 C
44) 13.4.1 E
45) 13.1.1 A
46) 13.1.3 C
47) 13.3.1 D
48) 13.1.2 B
49) 14.1.2 B
50) 14.1.2 A
51)15.1.3 A
52) 16.1.2 A
53) 16.1.4 C
54) 16.1.5 D
55) 3.1.9 D
56) 16.1.3 B
Contours every 100m
Fault, ticks on down thrown side

Figure 1

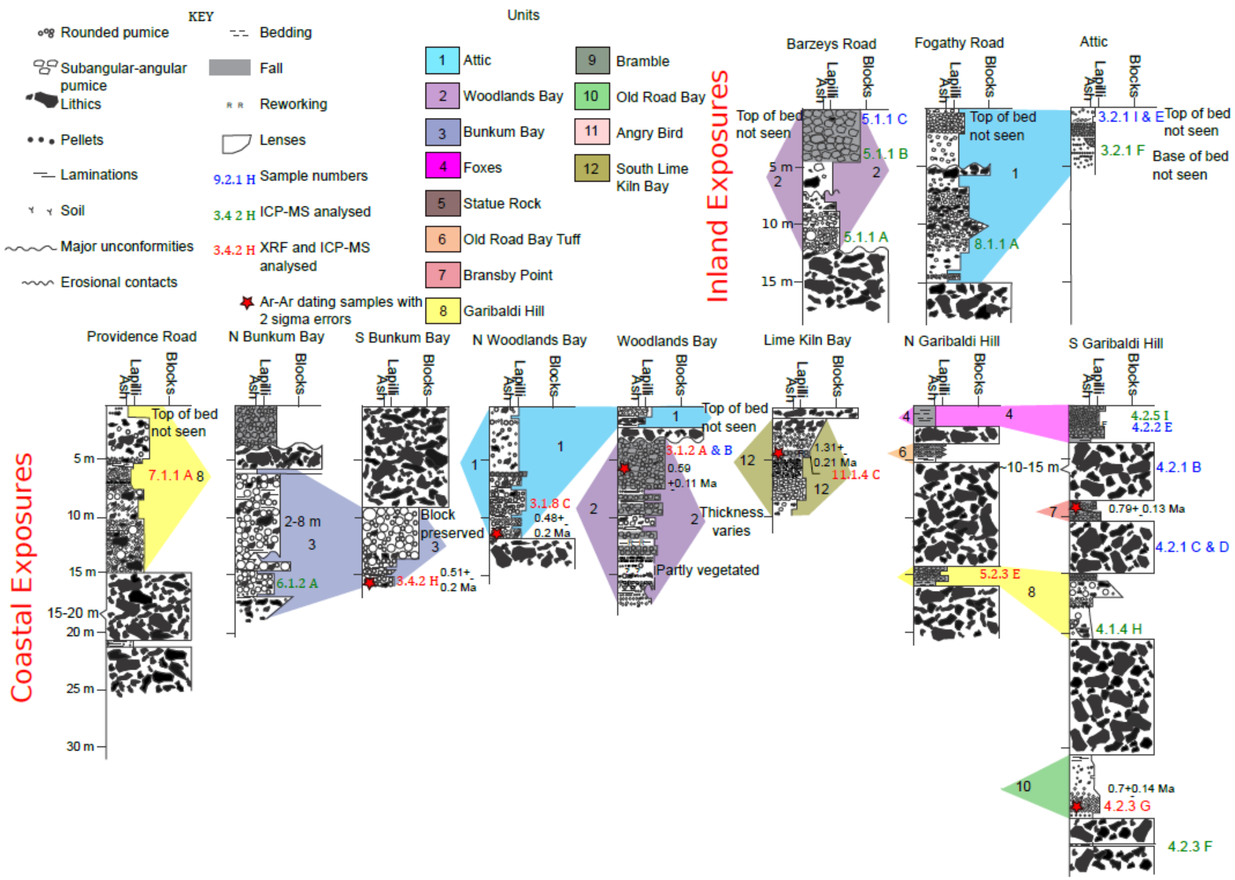

KEY
Rounded pumice
Subangular-angular pumice
Lithics
Pellets
Laminations
Soil
Major unconformities
Erosional contacts
Bedding
Fall
Reworking
Lenses
9.2.1 H Sample numbers
3.4 2 H ICP-MS analysed
3.4.2 H XRF and ICP-MS analysed
Ar-Ar dating samples with 2 sigma errors
Units
1 Attic
2 Woodlands Bay
3 Bunkum Bay
4 Foxes
5 Statue Rock
6 Old Road Bay Tuff
7 Bransby Point
8 Garibaldi Hill
9 Bramble
10 Old Road Bay
11 Angry Bird
12 South Lime Kiln Bay
Inland Exposures
Barzeys Road
Fogathy Road
Attic
Coastal Exposures
Providence Road
N Bunkum Bay
S Bunkum Bay
N Woodlands Bay
Woodlands Bay
Lime Kiln Bay
N Garibaldi Hill
S Garibaldi Hill
Ash
Lapilli
Blocks
Top of bed not seen
Base of bed not seen
Block preserved
Thickness varies
Partly vegetated
5 m
10 m
15 m
15-20 m
20 m
25 m
30 m
2-8 m
10-15 m
5.1.1 C
5.1.1 B
5.1.1 A
8.1.1 A
3.2.1 I & E
3.2.1 F
7.1.1 A
6.1.2 A
3.4.2 H
0.51± 0.2 Ma
3.1.8 C
0.48± 0.2 Ma
3.1.2 A & B
0.59 ±0.11 Ma
1.31± 0.21 Ma
11.1.4 C
5.2.3 E
4.2.5 I
4.2.2 E
4.2.1 B
0.79± 0.13 Ma
4.2.1 C & D
4.1.4 H
0.7±0.14 Ma
4.2.3 G
4.2.3 F


Figure 2

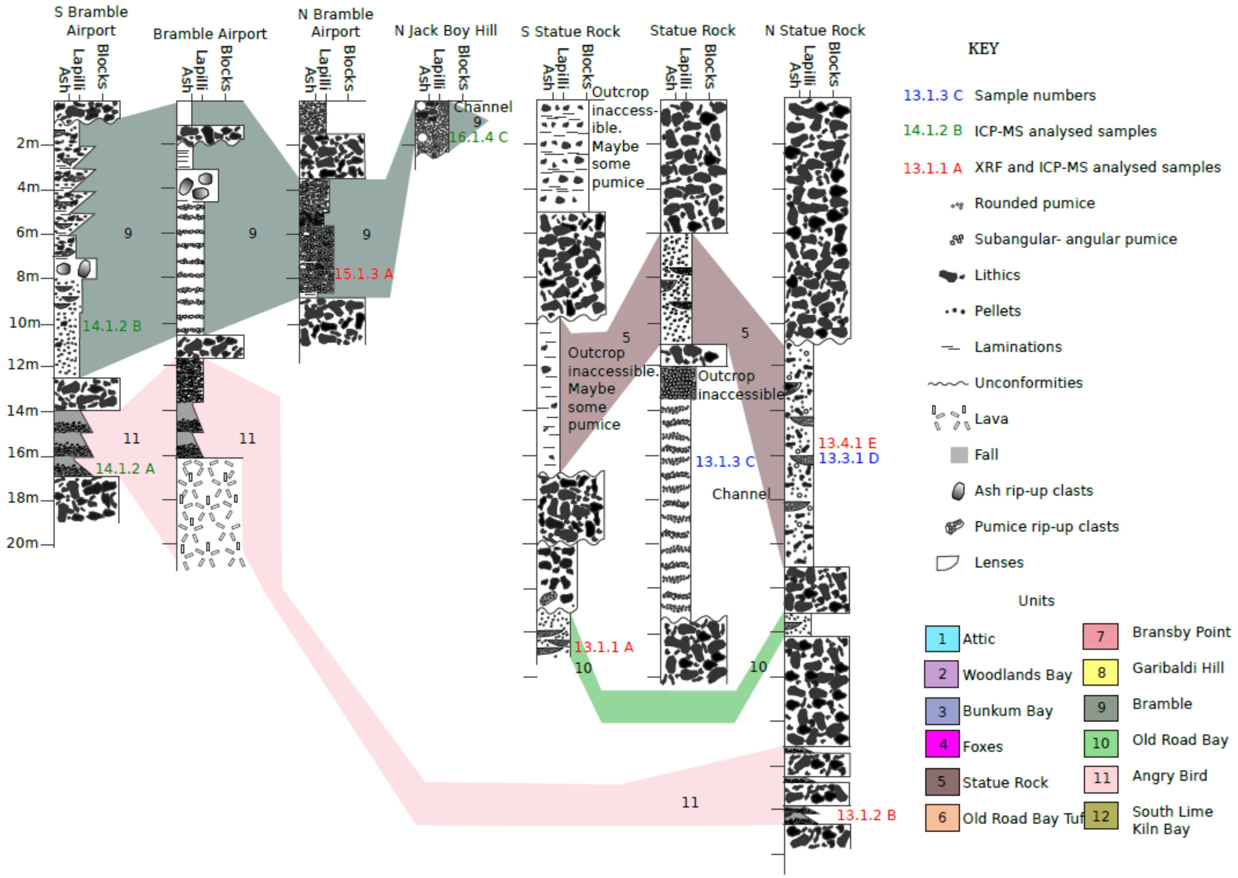

S Bramble Airport
Bramble Airport
N Bramble Airport
N Jack Boy Hill
S Statue Rock
Statue Rock
N Statue Rock
Ash Lapilli Blocks
2m
4m
6m
8m
10m
12m
14m
16m
18m
20m
Channel
16.1.4 C
15.1.3 A
14.1.2 B
14.1.2 A
Outcrop inaccess-ible. Maybe some pumice
Outcrop inaccessible. Maybe some pumice
Outcrop inaccessible
13.1.3 C
13.4.1 E
13.3.1 D
Channel
13.1.1 A
13.1.2 B
KEY
13.1.3 C Sample numbers
14.1.2 B ICP-MS analysed samples
13.1.1 A XRF and ICP-MS analysed samples
Rounded pumice
Subangular- angular pumice
Lithics
Pellets
Laminations
Unconformities
Lava
Fall
Ash rip-up clasts
Pumice rip-up clasts
Lenses
Units
1 Attic
2 Woodlands Bay
3 Bunkum Bay
4 Foxes
5 Statue Rock
6 Old Road Bay Tuff
7 Bransby Point
8 Garibaldi Hill
9 Bramble
10 Old Road Bay
11 Angry Bird
12 South Lime Kiln Bay


Figure 3


N 16.77051, W 62.16901
Angry Bird pumice

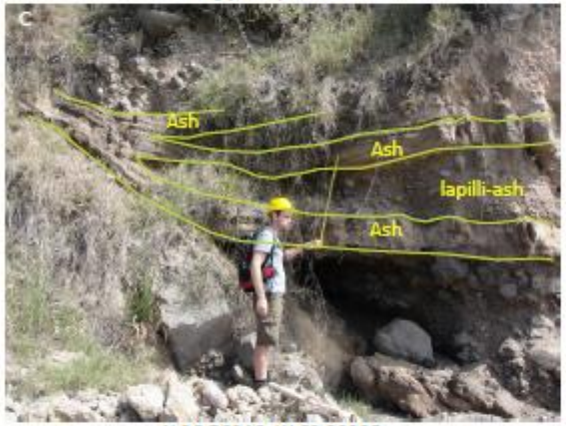


N 16.76946, W 62.22195
Bunkum Bay pumice

N 16.75413, W 62.22226
Attic pumice


N 16.72365, W 62.24035
Bransby Point pumice


N 16.76298, W 62.22343
Woodlands pumice

Figure 4

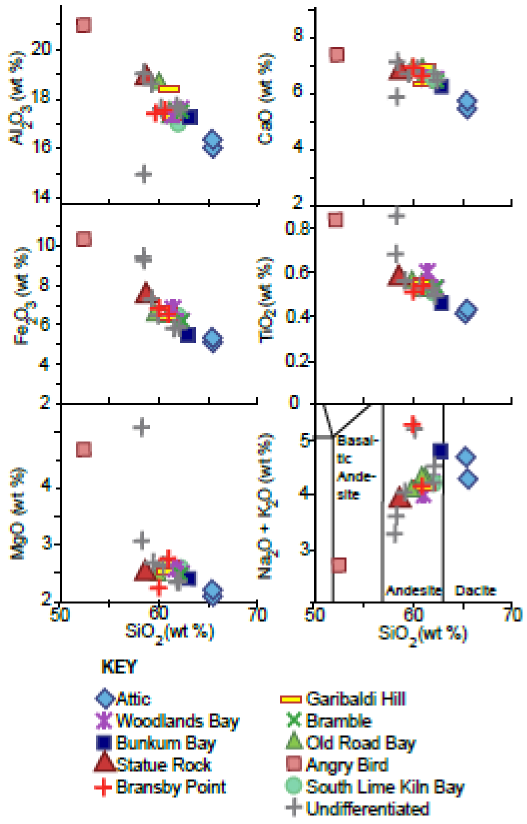

$Al_2O_3$ (wt %)
CaO (wt %)
$Fe_2O_3$ (wt %)
$TiO_2$ (wt %)
MgO (wt %)
$Na_2O + K_2O$ (wt %)
Basal-tic Ande-site
Andesite
Dacite
$SiO_2$ (wt %)
KEY
Attic
Woodlands Bay
Bunkum Bay
Statue Rock
Bransby Point
Garibaldi Hill
Bramble
Old Road Bay
Angry Bird
South Lime Kiln Bay
Undifferentiated


Figure 5

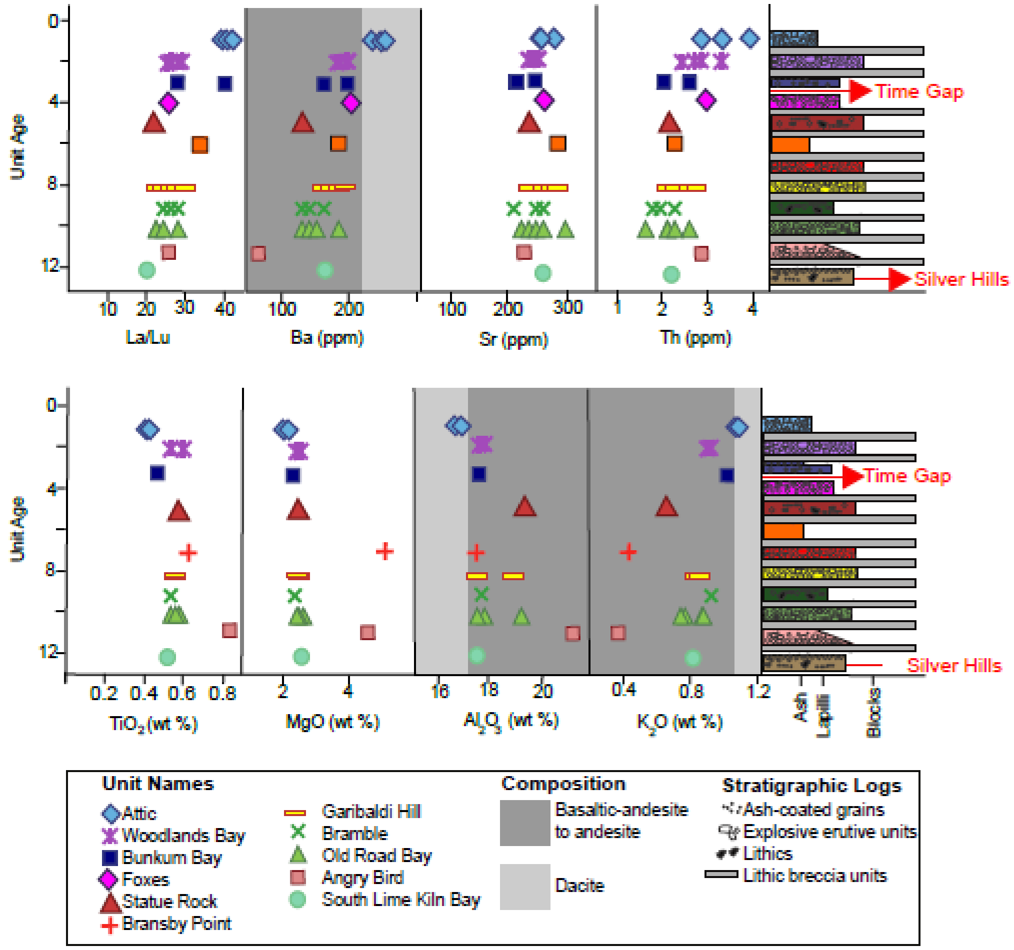

Unit Age
0
4
8
12
10 20 30 40
La/Lu
100 200
Ba (ppm)
100 200 300
Sr (ppm)
1 2 3 4
Th (ppm)
Time Gap
Silver Hills
0.2 0.4 0.6 0.8
TiO2 (wt %)
2 4
MgO (wt %)
16 18 20
Al2O3 (wt %)
0.4 0.8 1.2
K2O (wt %)
Ash
Lapilli
Blocks
Unit Names
Attic
Woodlands Bay
Bunkum Bay
Foxes
Statue Rock
Bransby Point
Garibaldi Hill
Bramble
Old Road Bay
Angry Bird
South Lime Kiln Bay
Composition
Basaltic-andesite to andesite
Dacite
Stratigraphic Logs
Ash-coated grains
Explosive erutive units
Lithics
Lithic breccia units


Figure 6

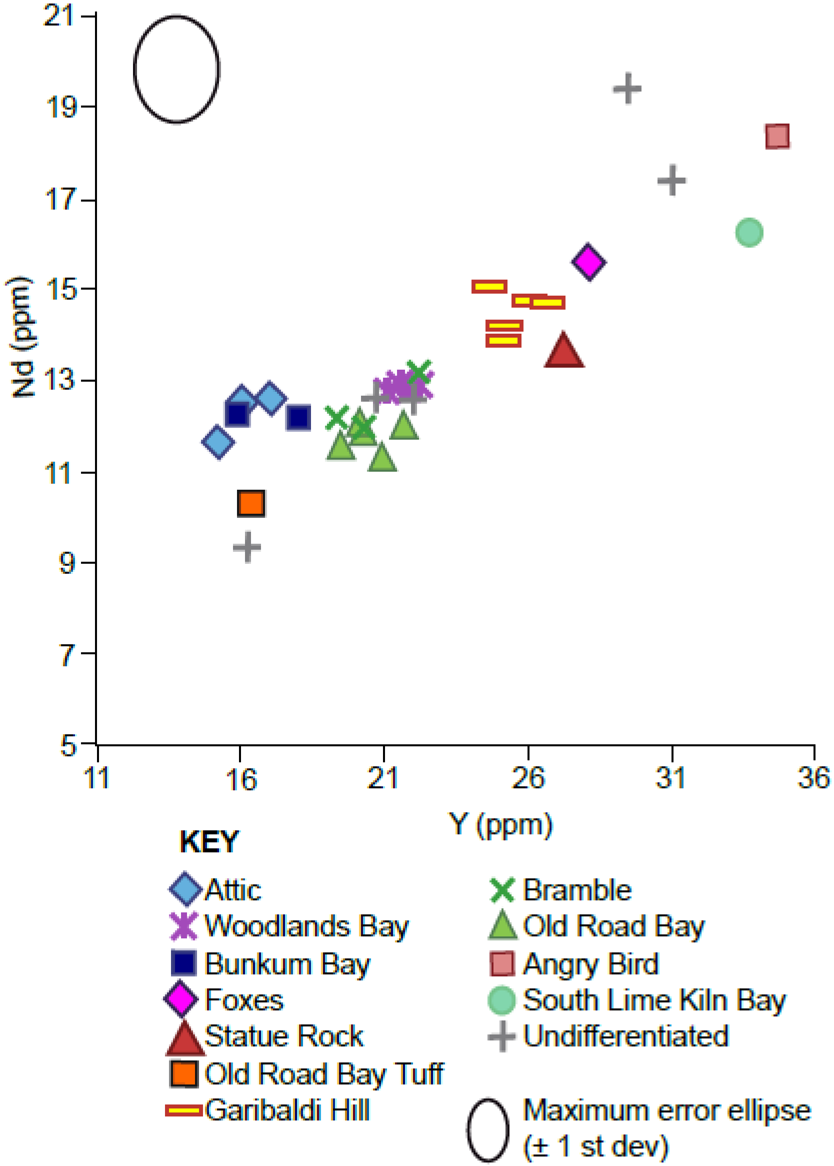

21
19
17
15
13
11
9
7
5
Nd (ppm)
11
16
21
26
31
36
Y (ppm)
KEY
Attic
Woodlands Bay
Bunkum Bay
Foxes
Statue Rock
Old Road Bay Tuff
Garibaldi Hill
Bramble
Old Road Bay
Angry Bird
South Lime Kiln Bay
Undifferentiated
Maximum error ellipse
(± 1 st dev)

Figure 7

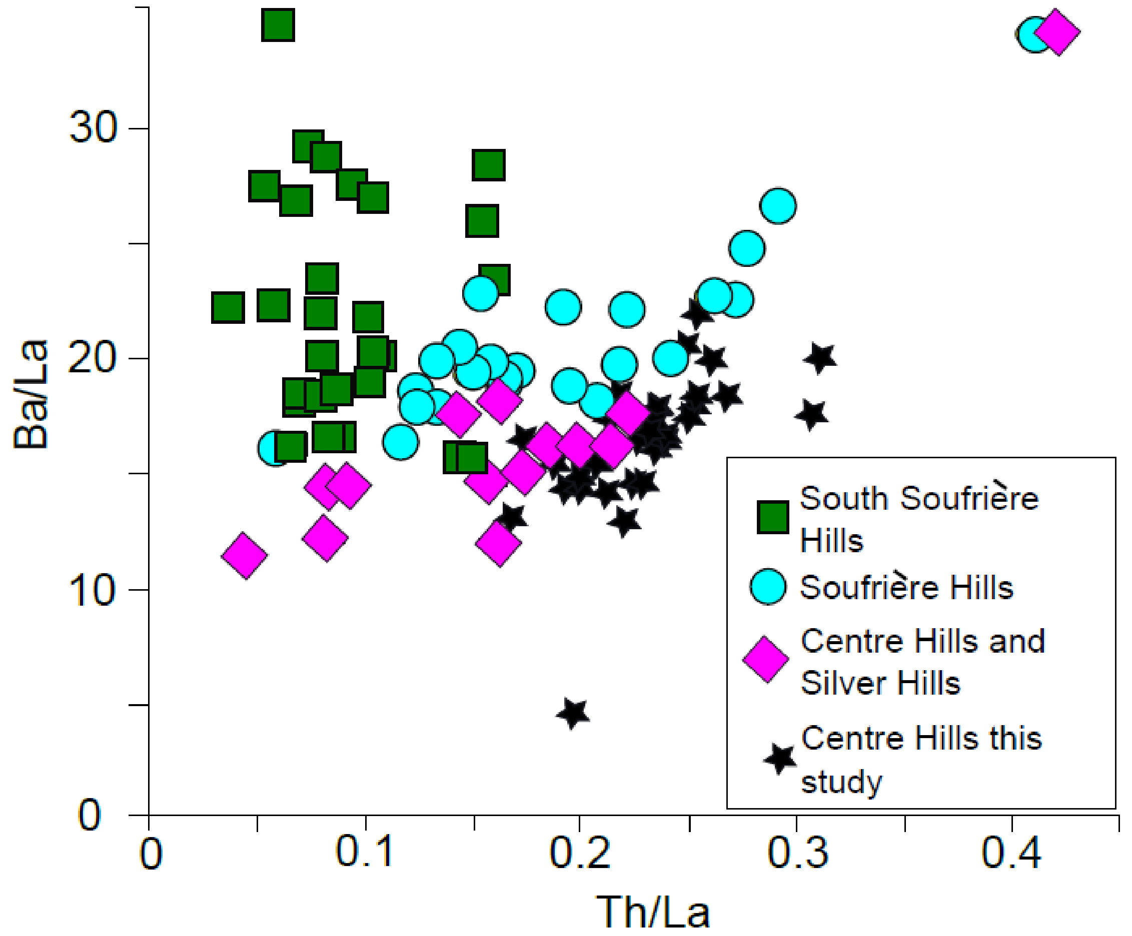

Ba/La
30
20
10
0
Th/La
0
0.1
0.2
0.3
0.4
South Soufrière Hills
Soufrière Hills
Centre Hills and Silver Hills
Centre Hills this study


Figure 8

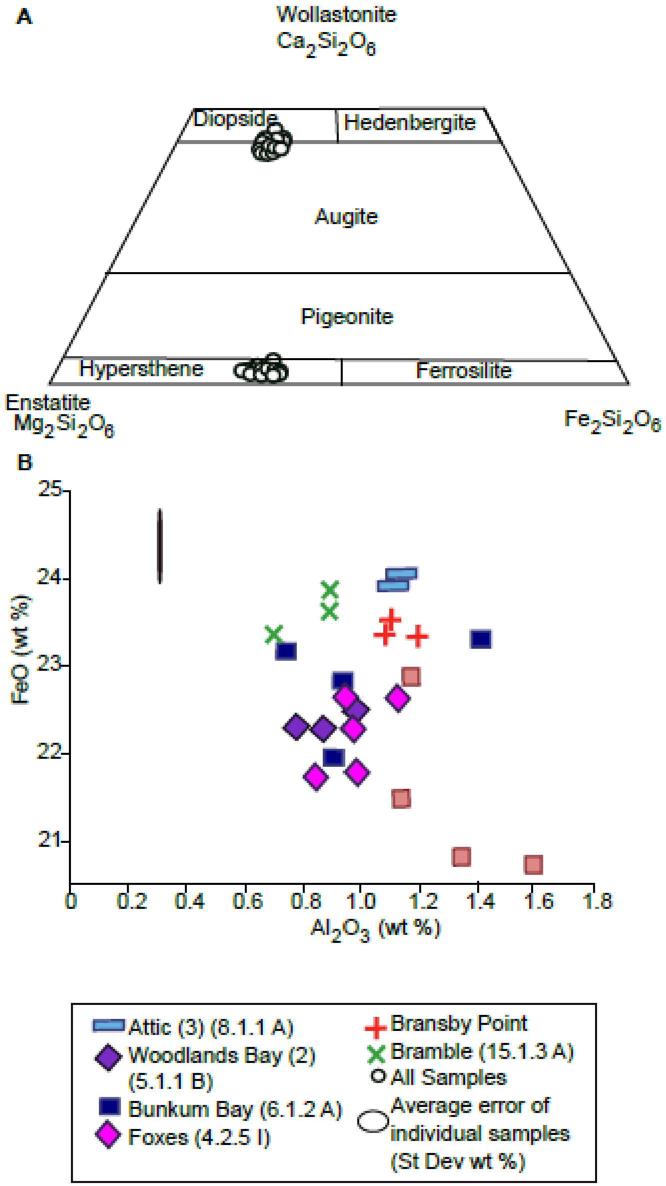
A
Wollastonite
$Ca_2Si_2O_6$
Diopside
Hedenbergite
Augite
Pigeonite
Hypersthene
Ferrosilite
Enstatite
$Mg_2Si_2O_6$
$Fe_2Si_2O_6$
B
FeO (wt %)
$Al_2O_3$ (wt %)
Attic (3) (8.1.1 A)
Woodlands Bay (2) (5.1.1 B)
Bunkum Bay (6.1.2 A)
Foxes (4.2.5 I)
Bransby Point
Bramble (15.1.3 A)
All Samples
Average error of individual samples (St Dev wt %)

Figure 9

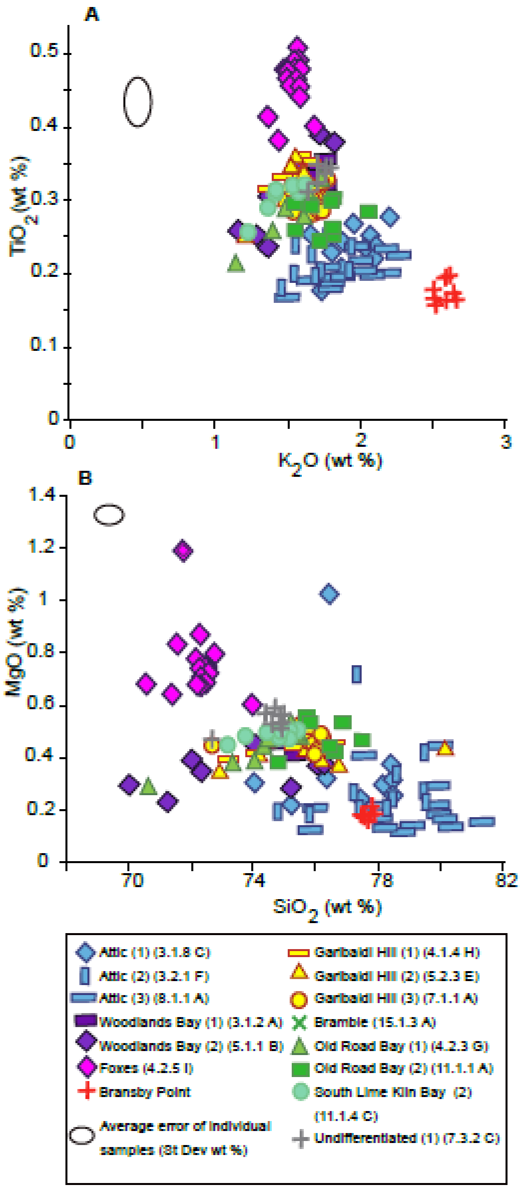
A
0.5
0.4
0.3
0.2
0.1
0
TiO2 (wt %)
0
1
2
3
K2O (wt %)
B
1.4
1.2
1
0.8
0.6
0.4
0.2
0
MgO (wt %)
70
74
78
82
SiO2 (wt %)
Attic (1) (3.1.8 C)
Attic (2) (3.2.1 F)
Attic (3) (8.1.1 A)
Woodlands Bay (1) (3.1.2 A)
Woodlands Bay (2) (5.1.1 B)
Foxes (4.2.5 I)
Bransby Point
Average error of individual samples (St Dev wt %)
Garibaldi Hill (1) (4.1.4 H)
Garibaldi Hill (2) (5.2.3 E)
Garibaldi Hill (3) (7.1.1 A)
Bramble (15.1.3 A)
Old Road Bay (1) (4.2.3 G)
Old Road Bay (2) (11.1.1 A)
South Lime Kiln Bay (2) (11.1.4 C)
Undifferentiated (1) (7.3.2 C)

Figure 10

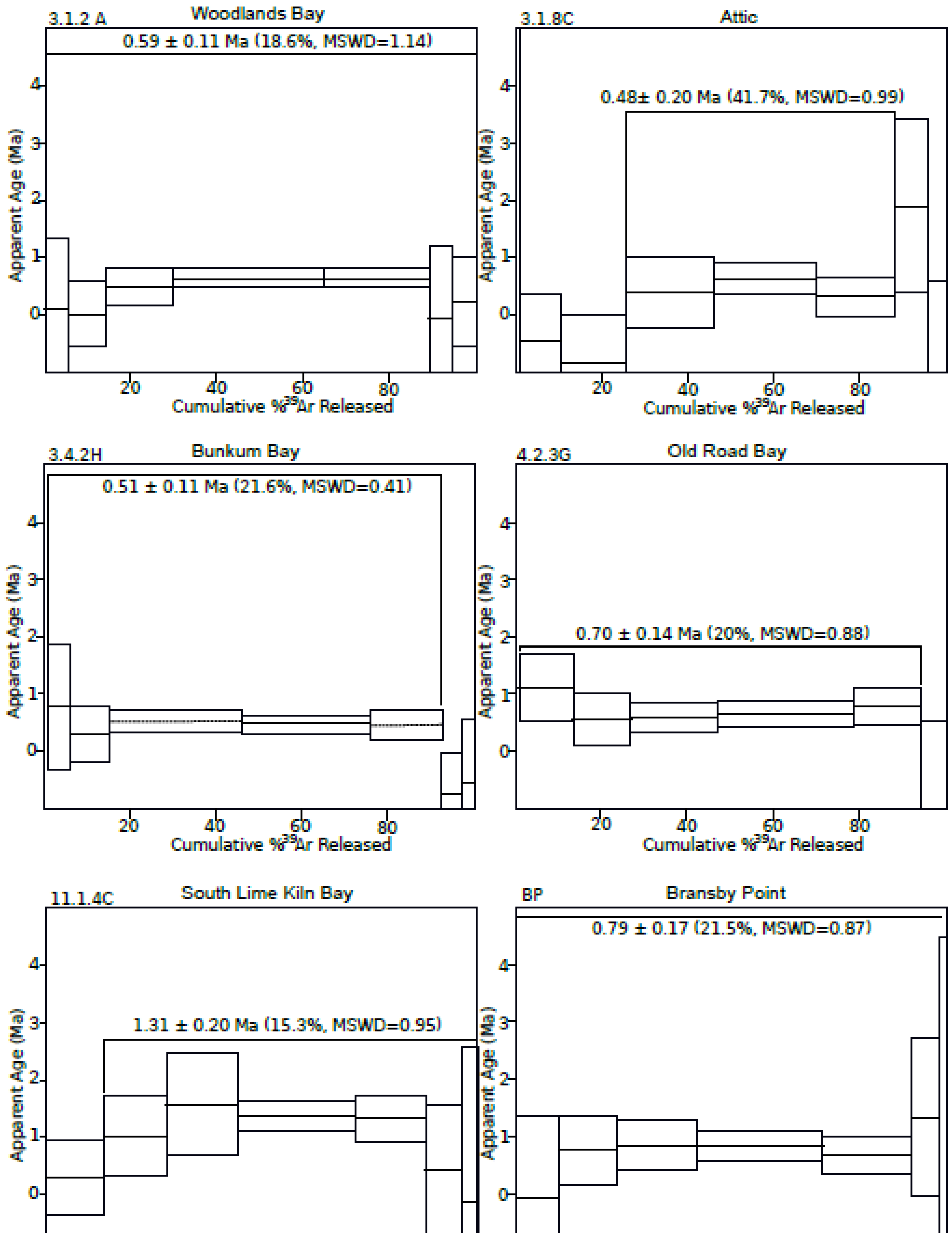
3.1.2 A
Woodlands Bay
0.59 ± 0.11 Ma (18.6%, MSWD=1.14)
Apparent Age (Ma)
Cumulative %39Ar Released
3.1.8C
Attic
0.48± 0.20 Ma (41.7%, MSWD=0.99)
3.4.2H
Bunkum Bay
0.51 ± 0.11 Ma (21.6%, MSWD=0.41)
4.2.3G
Old Road Bay
0.70 ± 0.14 Ma (20%, MSWD=0.88)
11.1.4C
South Lime Kiln Bay
1.31 ± 0.20 Ma (15.3%, MSWD=0.95)
BP
Bransby Point
0.79 ± 0.17 (21.5%, MSWD=0.87)

Figure 11

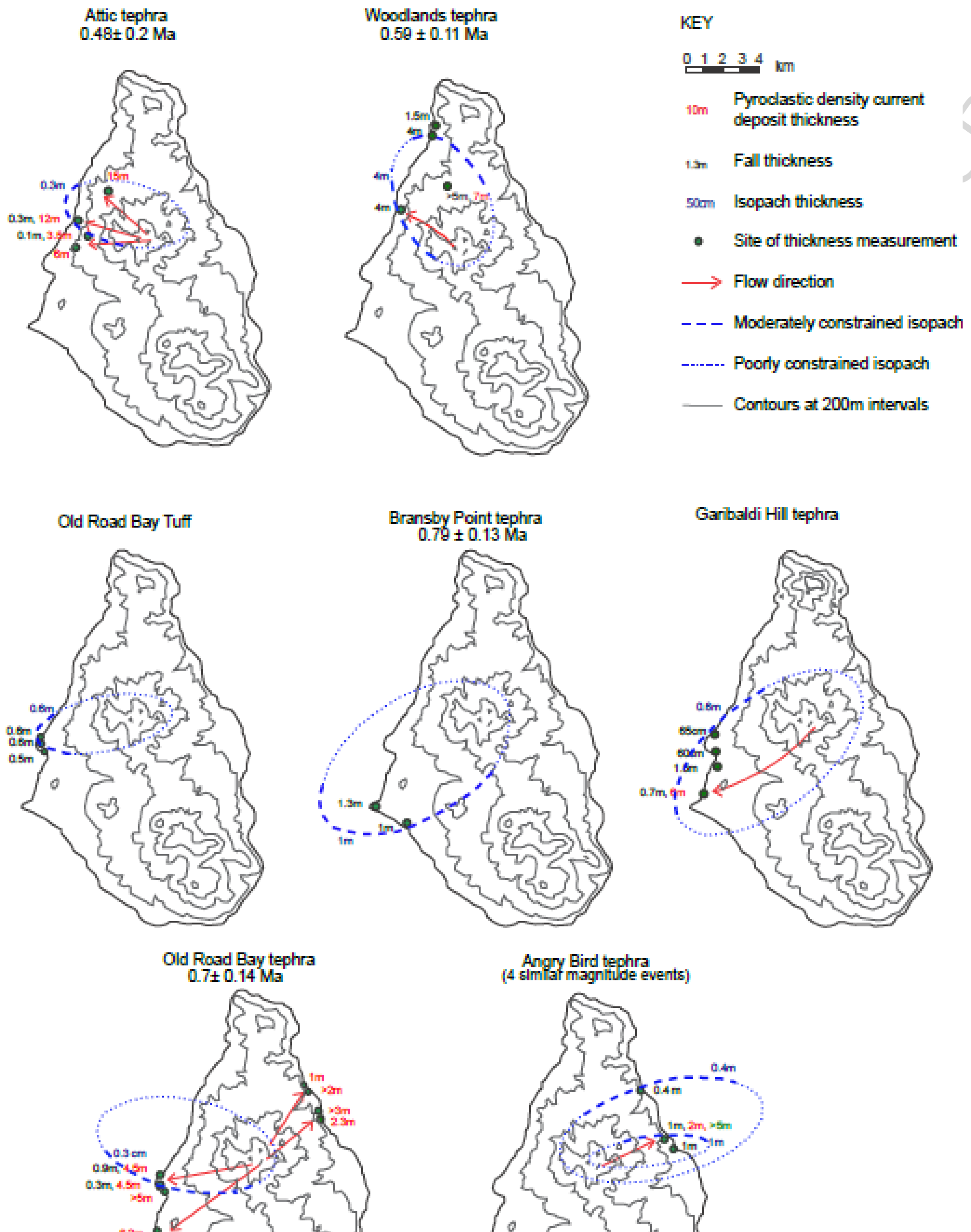
Attic tephra
0.48± 0.2 Ma
Woodlands tephra
0.59 ± 0.11 Ma
KEY
0 1 2 3 4 km
10m Pyroclastic density current deposit thickness
1.3m Fall thickness
50cm Isopach thickness
Site of thickness measurement
Flow direction
Moderately constrained isopach
Poorly constrained isopach
Contours at 200m intervals
Old Road Bay Tuff
Bransby Point tephra
0.79 ± 0.13 Ma
Garibaldi Hill tephra
Old Road Bay tephra
0.7± 0.14 Ma
Angry Bird tephra
(4 similar magnitude events)

Figure 12

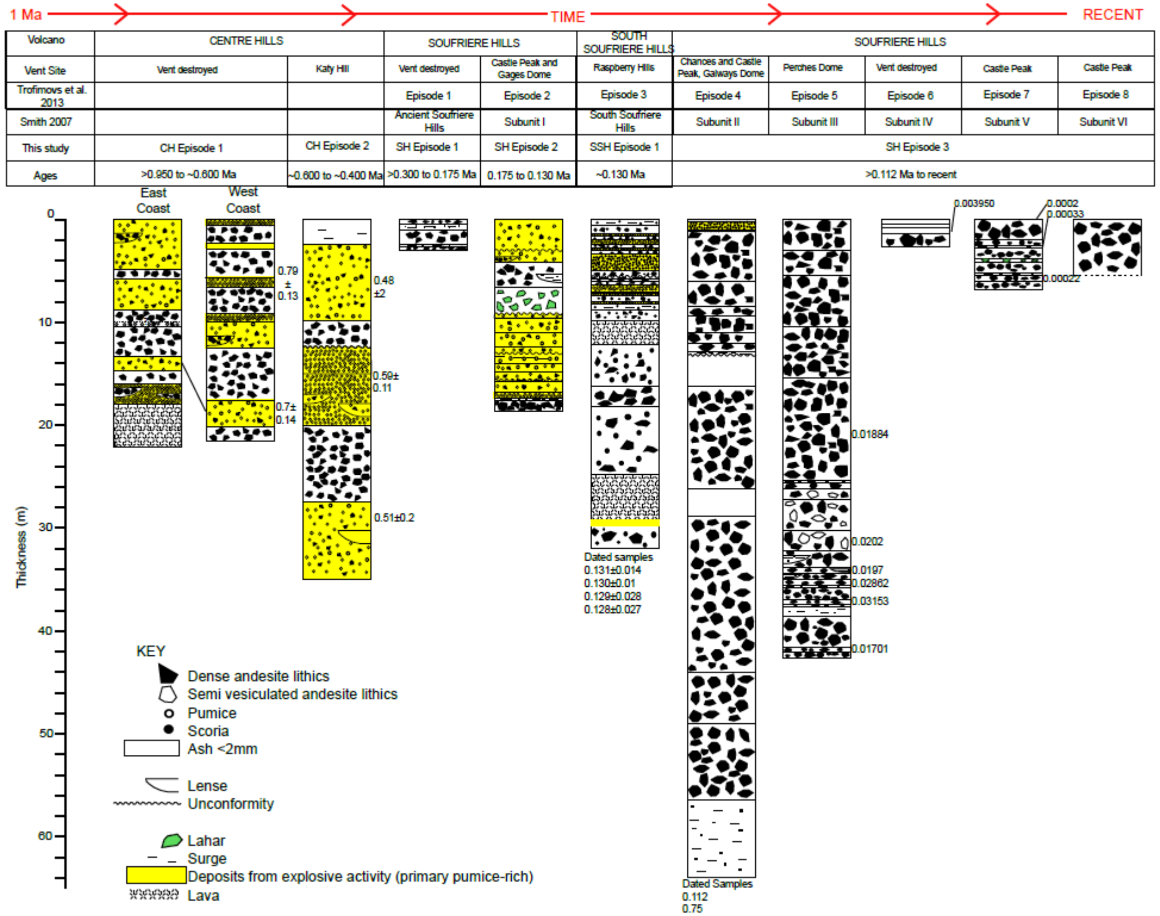
1 Ma
TIME
RECENT
Volcano
CENTRE HILLS
SOUFRIERE HILLS
SOUTH SOUFRIERE HILLS
SOUFRIERE HILLS
Vent Site
Vent destroyed
Katy Hill
Vent destroyed
Castle Peak and Gages Dome
Raspberry Hills
Chances and Castle Peak, Galways Dome
Perches Dome
Vent destroyed
Castle Peak
Castle Peak
Trofimovs et al. 2013
Episode 1
Episode 2
Episode 3
Episode 4
Episode 5
Episode 6
Episode 7
Episode 8
Smith 2007
Ancient Soufriere Hills
Subunit I
South Soufriere Hills
Subunit II
Subunit III
Subunit IV
Subunit V
Subunit VI
This study
CH Episode 1
CH Episode 2
SH Episode 1
SH Episode 2
SSH Episode 1
SH Episode 3
Ages
>0.950 to ~0.600 Ma
~0.600 to ~0.400 Ma
>0.300 to 0.175 Ma
0.175 to 0.130 Ma
~0.130 Ma
>0.112 Ma to recent
East Coast
West Coast
Thickness (m)
0.79 ± 0.13
0.7± 0.14
0.48 ±2
0.59± 0.11
0.51±0.2
Dated samples
0.131±0.014
0.130±0.01
0.129±0.028
0.128±0.027
Dated Samples
0.112
0.75
0.01884
0.0202
0.0197
0.02862
0.03153
0.01701
0.003950
0.0002
0.00033
0.00022
KEY
Dense andesite lithics
Semi vesiculated andesite lithics
Pumice
Scoria
Ash <2mm
Lense
Unconformity
Lahar
Surge
Deposits from explosive activity (primary pumice-rich)
Lava

Figure 13

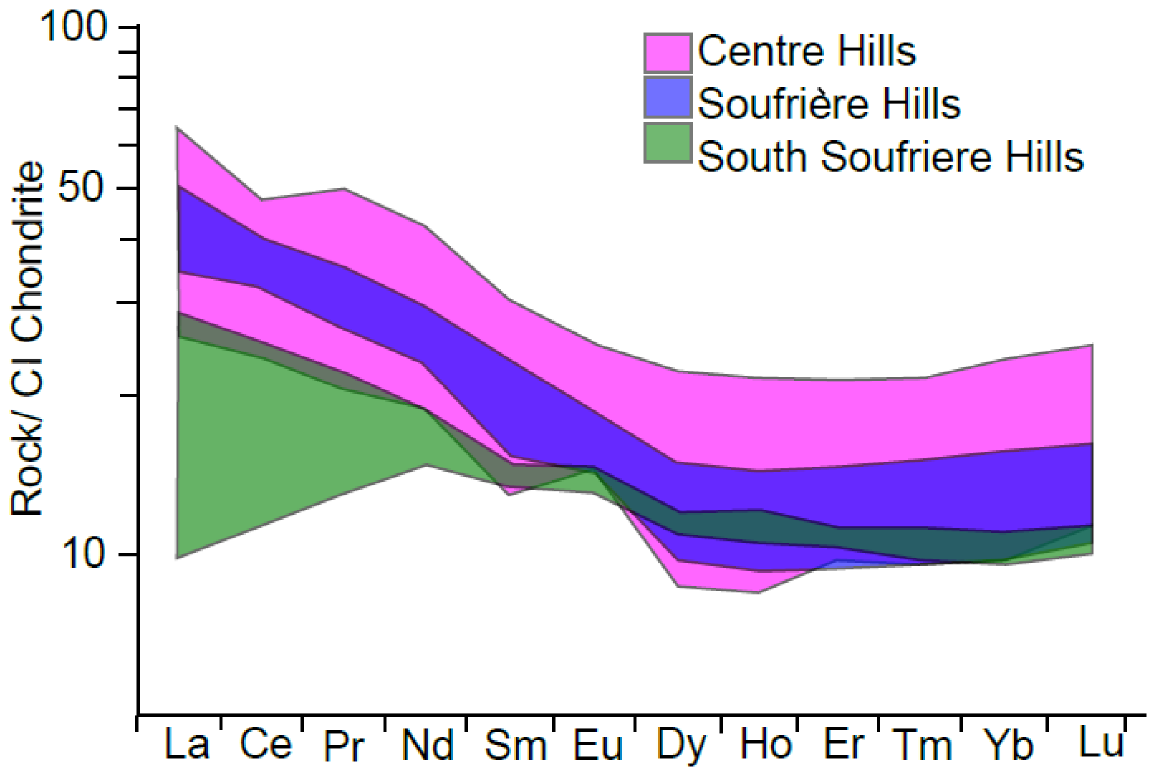
100
50
10
Rock/ CI Chondrite
Centre Hills
Soufrière Hills
South Soufriere Hills
La
Ce
Pr
Nd
Sm
Eu
Dy
Ho
Er
Tm
Yb
Lu

Figure 14

Highlights

- Presentation of a comprehensive subaerial stratigraphy of Montserrat spanning 1 Ma
- Eruptive products from both active centres are compositionally similar
- Activity at the older centre tended towards more sustained explosive eruptions
- Variation may be due to differences in magma ascent, temperature or storage